ГЕОЛОГИЯ, ПОИСКИ И РАЗВЕДКА ТВЁРДЫХ ПОЛЕЗНЫХ ИСКОПАЕМЫХ, МИНЕРАГЕНИЯ

УДК 552.321.6+553.46

Compositional Variation of Chrome Spinels in the Ore-bearing Zones of the Kraka Ophiolite and the Chromitite Origin

D.E. Saveliev[a], I.A. Blinov[b]
[a] Institute of Geology, Ufa Scientific Center, Russian Academy of Sciences, 16/2 Karl Marks Str., Ufa 450077, Russia. E-mail: savl71@mail.ru
[b] Institute of Mineralogy, Russian Academy of Sciences (Ural Branch), Ilmen Reserve, Miass 456301, Russia. E-mail: ivan_a_blinov@mail.ru
(Paper accepted 10/10.16)

The article considers a chemical variation of accessory and ore-forming chrome spinels from the Kraka ultramafic massif at the different scales, from the deposit to the thin section. A correlation analysis of compositional and structural features of ultramafic rocks and ores was performed. The ultramafic rocks and chromitites in the studied massif show the distinct deformation structures and tectonite olivine fabric. A typical chemical gap (i.e. Cr#=Cr/(Cr+Al)) was observed between peridotite, on the one hand, and dunite and chromitite, on the other hand, on the scale of deposits and ore-bearing zones. The location and size of this gap depend on the type of deposit. The gap becomes wider from the disseminated tabular bodies to the typical podiform ones. It has been found that in the thin initial dunite veinlets in peridotite the chrome spinels chemistry changes gradually and there is no Cr# gap between peridotite and dunite. The dunite venlets show a strong olivine fabric, which is an evidence of their high-temperature plastic flow origin. It has been revealed that new chrome spinel grains previously formed as rods or needles and then coarsened. We explained this observation as the result of impurity segregation, coalescence and spheroidization induced by the plastic deformation of olivine. It is inferred that a solid crystal flow is the main requirement for the dunite and chromitite body formation in the Kraka ophiolite massif. In the solid stream, the mineral phase separation takes place. For example, olivine and orthopyroxene grains of parental peridotite separate from one another, and weaker (more mobile) olivine grains form dunite bodies in which chromitite appears as a result of impurity segregation.
Key words: *chrome spinel; ophiolite; ultramafic rocks; plastic flow; podiform chromitite*
DOI: 10.17072/psu.geol.16.2.130

Introduction

Chrome spinel is an important petrological indicator because its chemistry is sensitive to the changes of external conditions (temperature, pressure, stress) (Dick, Bullen, 1984; Irvine, 1965). Chemistry of chrome spinel grains of ophiolite ultramafic rocks varies over a broad range. Similar compositional variations occur in spinels from ultramafic rocks located in different «present-day» tectonic settings (Barnes, Roeder, 2001). An interpretation of original tectonic setting of mantle ultramafic rocks exposed in the ancient fold belts bases on the comparison of its spinel compositions with those from typical «present-day-tectonic-setting» ultramafic rocks (e.g. Kelemen et al., 1992; 1995; Roberts, 1988; Zhou, Robinson, 1994).

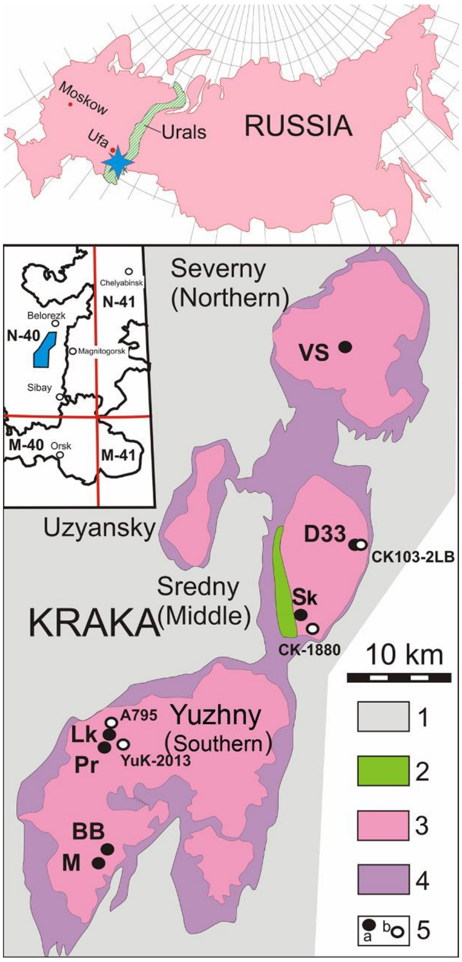

Fig. 1. *Schematic geological map of Kraka ophiolite and location of study areas: 1 – country rocks (from Ordovician to Devonian) of Zilairskaya megazone, northern part; 2 – crust section (gabbro, clinopyroxenite, wehrlite); 3 – mantle section (predominantly peridotite and less dunite); 4 – tectonized serpentinite; 5 – studied deposits and occurrences (a), and outcrops (b)*

However, a lot of ophiolite complexes show different spinel chemistry between peridotite, on the one hand, and dunite and chromitite, on the other hand (Pavlov et al., 1968; Perevozchikov, 1995). In addition, part of ultramafic massifs has the contrasting (bimodal) composition of chrome spinels. They are subdivided into the metallurgical and refractory types. These complexes are Kempirsay, Ray-Iz (the Urals), Zambales (the Philippines), Mayarí-Cristal (Cuba), Sakhakot-Quila (Pakistan). In other massifs, all deposits belong to a single chemical type. The Kraka massifs can be attributed to complexes where most of chrome deposits and occurrences are constituted by chromite grains containing more than 50% Cr_2O_3 (Saveliev et al., 2008).

Most of researchers who have studied the chemical distinctions of chrome spinel in ophiolite ultramafic rocks during the last twenty years believe that they are the result of tectonic settings change in a certain mantle volume (at present = «massif»). In spite of the abundance of works on this problem, in which this opinion is generally accepted, we do not think that it has been conclusively proved. Our main arguments are: 1) absence of distinct geological criteria to separate non-contemporaneous (=of different tectonic setting) peridotite and dunite bodies, 2) presence of a broad chemical range of spinels in a small volume (several meters of size) (Saveliev, Blinov, 2015; Saveliev et al., 2014). Here we present some new data on the accessory and ore-forming spinel chemistry from the different chrome ore occurrences of Kraka. These data were obtained at different scales, from several mm to tens of meters. Based on obtained results, we suggest a new interpretation of its origin mechanism.

Objects and methods of study

Spinel chemistry was studied on the several sites of Sredny (Middle) and Yuzhny (Southern) Kraka massifs (Fig. 1). The most studied areas are chromitite-bearing zones (chromitite occurrences or deposits) with quite simple framework. They contain some disseminated and/or massive ores enveloped by dunite bodies with variable thickness. The wall rock is commonly peridotite with different amount of orthopyroxene (10-30%) and diopside (0-7%). The main analytical method used to study chrome spinels and rock-forming silicates was the Scanning Electron

Microscopy (SEM Vega 3 Tescan) with EDA (Oxford Instruments X-act) electron-probe microanalyzer. The standard reference materials were utilized to define the mineral chemical compositions. The olivine from the Sample MINM25-53, No 01-044 (Astimex Scientific Limited) was used for olivine and serpentine. Hematite (Elba, Italy) was used for Fe, O and periclase (synthetic single crystal) - for Mg in chromium spinel (in both cases from the Sample MINM25-53, No 01-044 (Astimex Scientific Limited). The same metals from the Sample № 1362 (Microanalysis Consultants LTD) were used as standards for Al, Cr, Ti and Ni elements in chromium spinel. Analytical conditions were 20-kV accelerating voltage, 12-nA probe current and 3-μm probe diameter. Ferric and ferrous iron was calculated assuming spinel stoichiometry. Some results of analyses are listed in Table 1 (chrome spinel) and Table 2 (olivine).

General geological setting

The Kraka ultramafic massif is located in the northern part of Zilairskaya megazone (megasynclinorium) of the Southern Urals western slope. Geological and structural features of these ultramafic rocks as well as relationships with surrounding rocks were considered in previous works (Kazantseva, Kamaletdinov, 1969; Senchenko, 1976). The internal structure of the massif and bulk-rock chemistry of different petrological units were described in (Denisova, 1990; Saveliev et al., 2008; Savelieva, 1987; Snachev et al., 2001). Here we present a very brief geological summary of mantle sections framework.

The Kraka ophiolite included four bodies: Severny (Northern), Uzyansky, Yuzhny (Southern) and Sredny (Middle). The first three of them are comprised of peridotites with subordinate dunites. It was found that a considerable amount of lherzolites is present in the Severny Kraka in contrast with the dunite bodies, which were virtually absent there. In the Uzyansky and Yuzhny Kraka, a banded dunite-harzburgite unit is widespread. Dunite bodies make up not more than 10% of its volume. The most complicated composition is characteristic for the Sredny Kraka. Its central and eastern parts consist of spinel peridotites (lherzotites and diopside-containing harzburgites). Rarely, these rocks include small dunite and spinel-plagioclase-lherzolite veins. Toward the south-west, the spinel peridotite shows a gradational transition to dunite-harzburgite unit, where dunite dominates. Further to the west, the dunite-harzburgite unit gives way to the crustal section (wehrlite, clinopyroxenite, and gabbro).

Results

General mineral chemistry of Kraka peridotites

The Kraka peridotites bulk chemistry was described in (Saveliev et al., 2008; Savelieva, 1987; Snachev et al., 2001). This massif was attributed to the «lherzolite-type» of ophiolite (Savelieva, 1987). The distribution of trace elements in the Kraka peridotites shows a weak depletion of mantle source. TR concentration is close to that in chondrite (Saveliev et al.). In the Kraka peridotites, an olivine composition changes in the range of Fa = 6–10 (dunite) to Fa = 10–12 (harzburgite and lherzolite). The ultramafic rocks show a wide range of compositional variations of the spinel ratio Cr/Al. The Cr# (Cr/(Cr+Al)) changes from 0.1–0.5 in lherzolites up to 0.6–0.7 in dunites. The Mg# = Mg/(Mg+Fe) is maximum in peridotites (0.6–0.9) and it decreases in dunites to 0.4–0.7. Accessory spinel grains have a very small TiO_2 content (0.1–0.2%). It increases slightly in the dunite spinel grains to 0.3%. Significant contents of other impurities were not found in spinels. In general, the Kraka peridotites are comparable with those characteristic for a subcontinental mantle root zone and/or a continental rifting mantle root zone (Chashchukhin et al., 2007; Saveliev et al., 2008). In contrast with that, the ore-forming chrome spinel contained within many small deposits and occurrences shows high Cr# chemistry. We will consider these in more detail below.

Table 1. *Average chemical composition of chromian spinels from ultramafic rocks of Kraka ophiolite*

	1	**2**	**3**	**4**	**5**	**6**	**7**	**8**	**9**	**10**	**11**	**12**	**13**	**14**	**15**	**16**	**17**	**18**	**19**
Sample #	YuK - 1679/1	YuK - 1697	YuK - 1679/5	YuK - 1679/3	YuK - 2012-02	YuK - 2012-03	YuK - 2012-04	YuK - 2012-05	YuK - 2012-06	YuK - 2015-02	YuK - 2015-03	YuK - 2015-04	YuK - 2015-05	YuK - 2015-06	YuK - 2015-07	YuK - 2015-08	YuK - 2015-09	YuK - 2015-09	YuK - 2015-10
Rock	Lc	Hb	Chrt	D	Hb	D	D	D	Chrt	D	Hb	D	Hb	D	D	Chrt	D	D	Hb
n	4	1	4	1	9	3	5	11	11	7	3	12	7	13	13	20	*15276h*	5	4
Al_2O_3	50.19	23.70	12.10	12.95	19.65	20.72	15.39	17.98	9.29	15.88	25.70	25.24	29.91	17.74	13.47	14.52	4.33	16.03	28.61
Cr_2O_3	18.58	46.48	54.29	52.88	48.85	47.11	52.06	49.55	61.08	52.27	43.98	43.40	39.65	50.43	55.98	54.50	57.41	51.31	39.60
MgO	16.88	11.49	10.37	9.95	12.73	11.12	10.43	11.20	12.52	10.69	12.92	11.78	13.10	12.42	10.56	13.82	4.58	11.64	13.84
FeO	14.08	18.05	22.87	23.70	18.07	20.41	21.32	20.73	16.56	20.78	17.22	19.11	17.05	19.07	19.67	16.95	33.15	20.03	17.74
TiO_2	–	0.08	0.11	0.00	0.03	–	0.17	0.07	0.12	0.25	–	0.06	0.03	0.16	0.29	0.25	0.53	0.26	0.10
MnO	0.04	0.21	0.22	0.38	0.35	0.38	0.39	0.30	0.39	–	–	–	–	–	–	–	–	0.04	–
NiO	0.24	–	0.03	0.13	0.03	–	–	–	0.02	–	–	0.02	0.03	–	–	–	–	–	–
V_2O_5	–	–	–	–	0.19	0.26	0.11	0.11	0.01	0.14	0.18	0.21	0.14	0.16	0.04	0.01	–	0.05	0.12
ZnO	–	–	–	–	0.10	–	0.13	0.08	–	–	–	0.18	0.11	0.02	–	–	–	–	–
Formula coefficients																			
Al	1.599	0.863	0.467	0.499	0.722	0.766	0.585	0.672	0.357	0.601	0.920	0.912	1.051	0.659	0.515	0.541	0.180	0.606	1.007
Cr	0.397	1.135	1.405	1.368	1.204	1.169	1.326	1.243	1.575	1.327	1.056	1.052	0.935	1.256	1.437	1.363	1.605	1.301	0.935
Mg	0.680	0.529	0.506	0.485	0.592	0.519	0.501	0.529	0.607	0.511	0.585	0.538	0.582	0.583	0.510	0.651	0.241	0.556	0.616
Fe^{+3}	0.005	–	0.132	0.128	0.064	0.057	0.071	0.076	0.063	0.057	0.014	0.023	0.003	0.075	0.041	0.090	0.190	0.083	0.050
Fe^{+2}	0.313	0.466	0.480	0.506	0.400	0.472	0.496	0.465	0.383	0.495	0.421	0.464	0.421	0.419	0.489	0.348	0.769	0.445	0.387
Ti	–	0.002	0.003	–	0.001	–	0.004	0.002	0.003	0.006	–	0.001	0.001	0.004	0.007	0.006	0.014	0.006	0.002
Mn	0.001	0.005	0.006	0.011	0.009	0.010	0.011	0.008	0.011	–	–	–	–	–	–	–	–	0.001	–
#Cr	0.20	0.57	0.75	0.73	0.63	0.60	0.69	0.65	0.82	0.69	0.53	0.54	0.47	0.66	0.74	0.72	0.90	0.68	0.48
#Mg	0.68	0.53	0.51	0.49	0.60	0.52	0.50	0.53	0.61	0.51	0.58	0.54	0.58	0.58	0.51	0.65	0.24	0.56	0.61

1-4 – Bolshoj Bashart and Menzhinsky, 5-9 – Pridorozhnoe, 10-19 – Laktybash, 20-25 – A-795; 26-32 – Y-2013; 33-34 – Verkhne-Saranginskoe, 35-37 – Sakseyskaya zone, 38-43 – CK-1880; 44-50 – Deposit #33; 51-56 – CK-103-2LB; "–" – concentration less than the location limit , n – number of analyses

Table 1. *Average chemical composition of chromian spinels from ultramafic rocks of Kraka ophiolite (continued)*

	20	21	22	23	24	25	26	27	28	29	30	31	32	33	34	35	36	37
Sample #	A-795-1	A-795-2	A-795-5	A-795-6	A-795-7	A-795-8	YuK - 2013-01	YuK - 2013-03	YuK - 2013-04	YuK - 2013-05	YuK - 2013-06	YuK - 2013-08	YuK - 2013-09	Cek-344	Cek-1776	PS-2008	CK-1108	CK-206-1
Rock	Hb	D	Hb	D	Hb	DHb	D	D	Hb	D	Chrt	Hb	Hb	Chrt	Hb-Lc	D	Chrt	Hb
n	1	1	1	1	1	1	5	3	4	1	13	3	5	5	9	9	8	1
Al_2O_3	45.91	19.64	45.39	27.78	34.63	31.96	11.01	22.46	34.91	12.46	10.42	25.01	30.35	12.04	27.60	10.08	9.08	31.94
Cr_2O_3	24.85	49.52	24.78	40.42	35.05	35.86	56.58	45.89	34.28	55.43	59.83	43.57	38.97	58.87	40.22	58.01	58.27	34.25
MgO	16.00	11.58	16.74	12.06	13.87	14.04	9.24	11.52	13.46	9.64	11.79	12.84	13.19	13.31	12.77	11.56	11.45	15.25
FeO	13.04	18.78	12.76	18.97	16.15	17.78	22.69	19.70	17.13	22.09	17.75	17.86	17.35	15.30	18.92	19.94	20.83	17.89
TiO_2	–	0.29	0.06	0.48	0.06	0.04	0.30	0.13	–	0.38	0.21	–	–	0.19	0.23	0.20	0.18	0.05
MnO	–	0.20	–	0.17	0.12	0.19	–	0.19	–	–	–	0.42	–	0.12	0.06	0.21	0.18	0.24
NiO	0.19	0.00	0.26	0.11	0.12	0.12	–	0.11	–	–	–	0.06	–	0.17	0.21	–	–	0.13
V_2O_5	–	–	–	–	–	–	–	–	0.21	–	–	0.24	0.11	–	–	–	–	0.26
ZnO	–	–	–	–	–	–	–	–	–	–	–	–	–	–	–	–	–	–
Formula coefficients																		
Al	1.494	0.727	1.473	0.992	1.189	1.109	0.430	0.822	1.201	0.482	0.401	0.899	1.065	0.455	0.981	0.389	0.353	1.101
Cr	0.542	1.230	0.539	0.968	0.808	0.834	1.484	1.127	0.791	1.439	1.542	1.050	0.917	1.492	0.961	1.501	1.517	0.792
Mg	0.658	0.542	0.687	0.544	0.602	0.616	0.456	0.533	0.586	0.471	0.573	0.583	0.585	0.636	0.575	0.563	0.561	0.665
Fe^{+3}	–	0.049	–	0.024	–	0.045	0.072	0.048	0.002	0.076	0.049	0.043	0.012	0.049	0.054	0.101	0.127	0.108
Fe^{+2}	0.301	0.439	0.294	0.454	0.393	0.387	0.550	0.459	0.416	0.522	0.430	0.408	0.418	0.356	0.417	0.434	0.432	0.318
Ti	–	0.007	0.001	0.011	0.001	0.001	0.007	0.003	–	0.009	0.005	–	–	0.004	0.005	0.005	0.005	0.001
Mn	–	0.005	–	0.004	0.003	0.005	–	0.005	–	–	–	0.011	–	0.003	0.001	0.006	0.005	0.006
#Cr	0.27	0.63	0.27	0.49	0.40	0.43	0.78	0.58	0.40	0.75	0.79	0.54	0.46	0.77	0.49	0.79	0.81	0.42
#Mg	0.69	0.55	0.70	0.55	0.60	0.61	0.45	0.54	0.58	0.47	0.57	0.59	0.58	0.64	0.58	0.56	0.56	0.68

Table 1. *Average chemical composition of chromian spinels from ultramafic rocks of Kraka ophiolite (end)*

	38	**39**	**40**	**41**	**42**	**43**	**44**	**45**	**46**	**47**	**48**	**49**	**50**	**51**	**52**	**53**	**54**	**55**	**56**
Sample #	CK-1880-01 Hb	CK-1880-01 DHb	CK-1880-02	CK-1880-03	CK-1880-04	CK-1880-05	CK-103-2LB	CK-103-2LZ	CK-103-3	CK-103-4	CK-9890	CK-103-2DA	CK-103-R	15131	15133	15133	15127	15127	15134
Rock	Hb	DHb	D	Hb	Hb	Hb	Lc	Lc	Lc-Hb	Lc-Hb	Lc-Hb	D	Chrt	Lc	DLc	DLc	D	D	D
n	7	16	13	7	2	8	4	10	6	2	1	4	7	3	8	*15133i*	10	*15127s*	7
Al_2O_3	26.96	25.35	14.41	26.13	22.44	26.33	45.35	53.42	43.48	26.99	29.77	12.23	9.31	39.56	38.72	22.59	37.04	46.58	35.74
Cr_2O_3	41.44	42.28	51.04	41.93	44.79	41.01	24.93	14.20	23.02	42.74	37.42	54.76	62.86	28.19	29.91	46.23	32.14	21.63	32.82
MgO	13.52	12.70	10.02	13.37	10.82	12.79	16.98	20.39	17.83	14.07	13.36	10.48	12.21	14.58	14.84	10.92	14.88	16.82	14.33
FeO	17.67	19.22	23.56	18.10	21.39	19.34	12.34	11.48	15.26	15.85	18.83	21.96	15.18	17.22	15.89	19.41	15.67	15.44	16.56
TiO_2	–	0.01	0.22	–	–	–	0.20	0.19	0.13	0.05	0.21	0.26	0.13	–	–	–	0.02	–	0.12
MnO	0.29	0.23	0.56	0.24	0.47	0.30	0.16	0.09	0.13	0.15	0.28	0.19	0.03	–	0.15	0.30	–	–	0.04
NiO	–	–	–	–	–	–	0.04	0.03	0.01	–	–	–	0.03	0.07	–	–	–	–	–
V_2O_5	0.03	0.22	0.19	0.23	0.09	0.23	–	0.12	0.16	0.16	0.14	0.12	–	–	–	–	–	–	0.04
ZnO	0.09	–	–	–	–	–	–	0.07	–	–	–	–	–	–	–	–	–	–	–
Formula coefficients																			
Al	0.957	0.910	0.548	0.931	0.826	0.942	1.469	1.651	1.413	0.955	1.047	0.471	0.356	1.332	1.306	0.833	1.256	1.499	1.222
Cr	0.987	1.019	1.312	1.004	1.105	0.984	0.543	0.294	0.502	1.014	0.883	1.415	1.630	0.637	0.678	1.144	0.731	0.467	0.754
Mg	0.607	0.577	0.482	0.603	0.503	0.578	0.696	0.797	0.732	0.629	0.594	0.511	0.593	0.621	0.633	0.509	0.638	0.684	0.620
Fe^{+3}	0.054	0.065	0.124	0.058	0.056	0.068	–	0.042	0.082	0.036	0.072	0.108	0.012	0.032	0.017	0.024	0.012	0.030	0.020
Fe^{+2}	0.385	0.417	0.508	0.394	0.496	0.415	0.284	0.205	0.261	0.357	0.390	0.481	0.405	0.377	0.362	0.482	0.363	0.320	0.379
Ti	–	–	0.006	–	–	–	0.004	0.004	0.003	0.001	0.005	0.006	0.003	–	–	–	0.001	–	0.003
Mn	0.007	0.006	0.016	0.006	0.012	0.008	0.004	0.002	0.003	0.004	0.007	0.005	0.001	–	0.004	0.008	–	–	0.001
#Cr	0.51	0.53	0.71	0.52	0.57	0.51	0.27	0.15	0.26	0.52	0.46	0.75	0.82	0.32	0.34	0.58	0.37	0.24	0.38
#Mg	0.61	0.58	0.49	0.60	0.50	0.58	0.71	0.80	0.74	0.64	0.60	0.52	0.59	0.62	0.64	0.51	0.64	0.68	0.62

Table 2. *Average chemical composition of olivine from ultramafic rocks of Kraka ophiolite*

	Sample	n	*Chemical composition (wt %%)*						*formula coefficients*					
			SiO_2	FeO	MnO	MgO	NiO	Sum.	Si	Fe	Mn	Mg	Ni	Fo
1	YuK-2012-02	5	41.30	7.77	0.07	50.47	0.38	100.00	1.00	0.16	0.004	1.83	0.01	0.92
2	YuK -2012-03	13	41.05	7.88	0.07	50.27	0.40	99.67	1.00	0.16	0.004	1.83	0.01	0.92
3	YuK -2012-04	4	41.10	7.85	0.08	50.29	0.37	99.73	1.00	0.16	0.004	1.83	0.01	0.92
4	YuK -2012-05	2	40.38	8.59	0.14	49.64	0.43	99.18	0.99	0.18	0.006	1.82	0.01	0.91
5	YuK -2012-11	4	41.28	7.18	–	50.77	0.47	99.71	1.00	0.15	–	1.84	0.01	0.93
6	YuK -2013-01	3	41.74	7.97	–	50.34	0.30	100.34	1.01	0.16	–	1.82	0.01	0.92
7	YuK -2013-03	2	41.52	8.52	0.09	49.65	0.34	100.12	1.01	0.17	0.005	1.81	0.01	0.91
8	YuK -2013-04	2	41.41	8.75	–	49.59	0.39	100.12	1.01	0.18	–	1.80	0.01	0.91
9	YuK -2013-05	1	41.69	7.60	0.22	50.67	0.29	100.48	1.01	0.15	0.01	1.83	0.01	0.92
10	YuK -2013-08	5	41.87	8.65	0.15	48.93	0.45	100.05	1.02	0.18	0.007	1.79	0.01	0.91
11	YuK -2013-09	6	41.54	8.12	0.03	50.11	0.35	100.15	1.01	0.16	0.002	1.82	0.01	0.92
12	YuK -2015-03	2	41.54	8.15	–	50.46	0.46	100.60	1.01	0.16	–	1.82	0.01	0.92
13	YuK -2015-04	4	41.58	8.28	0.10	50.07	0.32	100.35	1.01	0.17	0.005	1.81	0.01	0.92
14	YuK -2015-05	3	41.35	8.37	0.08	50.28	0.37	100.44	1.00	0.17	0.004	1.82	0.01	0.91
15	YuK -2015-06	6	41.51	7.41	–	50.60	0.39	99.91	1.01	0.15	–	1.83	0.01	0.92
16	YuK -2015-07	12	41.63	6.81	0.07	51.06	0.43	100.00	1.01	0.14	0.004	1.84	0.01	0.93
17	YuK -2015-09	2	40.82	7.65	0.10	50.10	0.41	99.06	1.00	0.16	0.006	1.83	0.01	0.92
18	YuK -2015-10	3	41.07	8.29	–	49.87	0.43	99.67	1.00	0.17	–	1.82	0.01	0.91
19	CK-1880-02	7	41.41	7.82	–	50.50	0.41	100.14	1.01	0.16	–	1.83	0.01	0.92
20	CK-1880-01 DHb	12	41.31	8.26	0.03	50.04	0.36	100.00	1.01	0.17	–	1.82	0.01	0.92
21	CK-1880-01 H	7	41.47	8.19	–	49.97	0.36	100.00	1.01	0.17	–	1.82	0.01	0.92
22	CK-1880-05	8	41.31	8.44	–	49.87	0.38	100.00	1.01	0.17	–	1.81	0.01	0.91
23	CK-1880-03	7	41.19	7.94	–	50.49	0.39	100.00	1.00	0.16	–	1.83	0.01	0.92
24	CK-1880-04	3	41.17	7.89	0.06	50.53	0.35	100.00	1.00	0.16	–	1.83	0.01	0.92
25	CK-98-90	1	41.93	10.22	0.17	49.48	0.23	102.02	1.01	0.21	0.004	1.78	0.004	0.90
26	CK-103-4	3	40.68	8.06	0.23	50.2	0.30	99.60	0.99	0.16	0.006	1.83	0.006	0.92
27	CK-103-3	2	40.76	9.60	0.2	48.54	0.50	99.66	1.00	0.20	0.005	1.78	0.01	0.90
28	CK-103-2LZ	9	40.72	10.05	0.23	48.29	0.34	99.71	1.00	0.21	0.006	1.78	0.007	0.90
29	CK-103-2DA	4	40.79	6.9	0.24	50.95	0.53	99.47	0.99	0.14	0.006	1.85	0.01	0.93
30	CK-103-2LB2	4	40.75	9.56	0.36	48.41	0.39	99.54	1.01	0.20	0.009	1.78	0.008	0.90
31	CK-103-2LB5	7	40.72	9.6	0.37	48.56	0.38	99.66	1.00	0.20	0.009	1.78	0.008	0.90
32	CK-103-2LB7	11	41.56	8.67	0.05	49.48	0.38	100.2	1.01	0.18	0.001	1.80	0.008	0.91
33	CK-103-2LB8	11	41.53	8.46	0.09	49.56	0.38	100.07	1.01	0.17	0.002	1.80	0.008	0.91

1-5 - Pridorozhnoe, 6-11 - YuK-2013; 12-18 - Laktybash, 19-24 – CK-1880; 25-33 – Deposit #33 and CK-103-2LB; "–" – concentration less than the location limit, n – number of analyses

Deposits and occurrences of chrome ore

Chrome ores occur in all four Kraka blocks; however, they are more abundant in the southwestern part of Sredny Kraka (Saksey-Klyuchevskaya area) and in the western part of Yuzhny Kraka (Apshakskaya and Bashartovskaya areas). The Kraka deposits were described in detail (Saveliev, 2012; Savelive et al., 2008), so here we consider particular characteristics, such as chrome spinel chemistry. Chrome ore is usually hosted by dunite. In some cases, it forms large bodies close to the Moho boundary, but, sometimes, the occurrences are presented by relatively small dunite lenses and tabular bodies (envelopes) within the mantle peridotites. According to the morphological classification of (Cassard et al., 1981), almost all occurrences are concordant, and disseminated ores predominate.

Bolshoy Bashart and Menzhinsky deposits

These deposits are located in the southwestern part of Yuzhny Kraka, 2 km from each other. Menzhinsky deposit is represented by a small number of extended (about 1000 m long) but thin (0.3–1.5 m) flat chromitite bodies. They are hosted by a flattened of 30 to 60 m thick dunite lens (Fig. 2a). The boundary between dunite and wall peridotite is sharp. The wall peridotite contains up to 30% of enstatite grains. At the same time, dunite envelopes include some harzburgite (10–15%) veinlets, which are parallel to dunite-chromitite banding. General banding and foliation are concordant and strike northwest, dipping to southeast at 45º. Chrome ore is dominantly dense-disseminated, and, rarely, irregularly disseminated or massive.

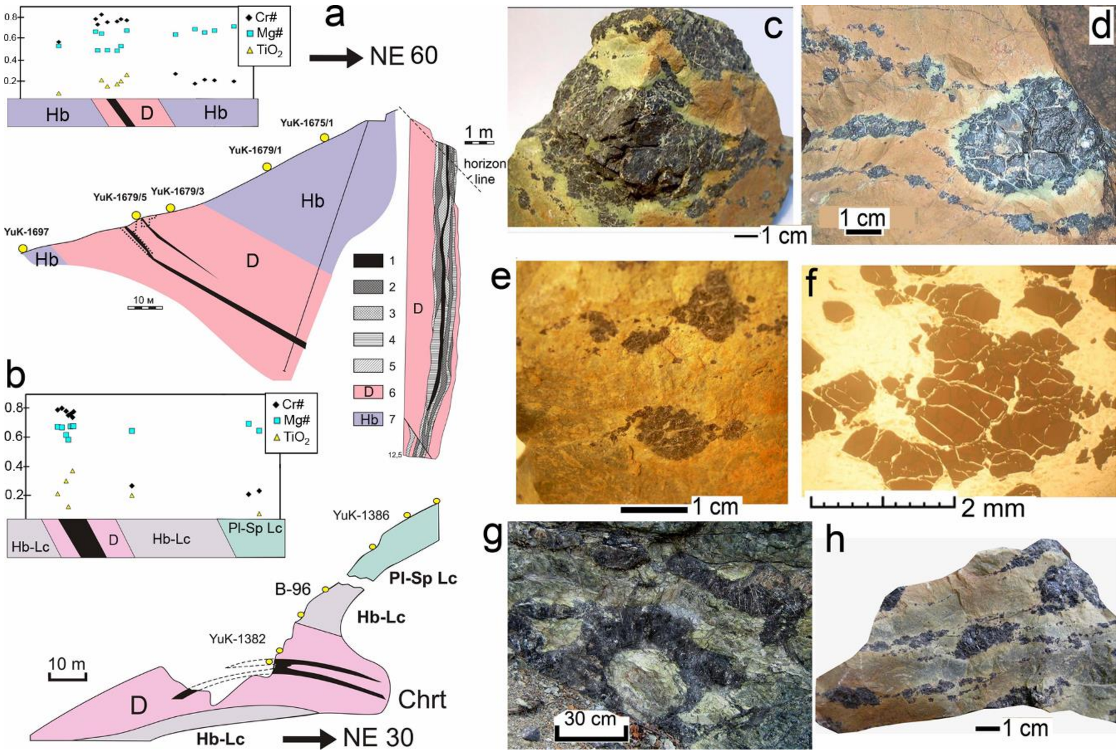

Fig. 2. *Cross-sections through Menzhinsky (a) and Bolshoj Bashart (b) deposits and structural features of chromitite (c – h): a – cross-sections through Menzhinsky deposit and compositional variations of spinels, 1–5 – chrome ore, 1 – massive (>80% chromite grains), 2–4 – disseminated with different chromite content (2 – 50–80 %, 3 – 30–50 %, 4 – 15–30 %), 5 – chromite-bearing dunite, 6 – dunite, 7 – peridotite; D – dunite, Chrt – chromitite, Hb-Lc – spinel peridotite between lherzolite and harzburgite in mineralogy, Pl-Sp Lc – plagioclase-spinel lherzolite; b – cross-sections through Bolshoj Bashart deposit; c – h – structural features of chromitite and their relationship with dunite; c, d, g, h – boudinage structures on different scale, e, f – «snow-ball» textures showing a mechanism of chromite grains segregation within solid plastic flow*

The Bolshoy Bashart deposit is composed of a few parallel chromitite veins transformed into a tree-like structure. The thickness of veins changes from 0.5 m up to 2.5 m. The ore veins are hosted by serpentinized dunite about 20 m thick (Fig. 2b). Dunite is surrounded by massive wall spinel peridotite with high concentration of enstatite (25–30%). The spinel-plagioclase peridotite outcrops are found a few dozen meters away from ore bodies. The chromitite-dunite ore-bearing zone lies almost flat, dipping gently (10–15°) to the north. Chrome ore is massive and dense-disseminated. It often exhibits deformation patterns, which is confirmed by a pull-apart texture, folding, boudinage of dunite within massive chromitite, boudinage of chromitite within dunite and snow-ball-texture in the chromite segregations (Fig. 2 c–h). Olivine grains from dunite show a well-marked fabric typical for mantle tectonites [46]. This means that dunite formed during a high-T plastic flow by the dislocation creep.

Chrome spinel composition changes in the wide range across both deposits. The spinel grains from the wall peridotite have Cr# = 0.2–0.3 and only a single sample shows its increase to 0.6. The spinels from the surrounding dunite and those from ore bodies have significantly higher Cr# (0.7–0.85). The number of Mg in spinels changes slightly along cross-section of both considered deposits. In the Menzhinsky deposit, it decreases gradually from wall peridotite (0.65–0.7) to dunite and chromitite (0.5–0.65). In the Bolshoj Bashart deposit, the Mg# is found to be constant at about 0.6–0.7. TiO_2 concentration in peridotite is usually lower than 0.1%, and only a few samples show higher value (up to 0.25%). It increases in the spinel grains from dunite and chromitite (0.1–0.4%).

Deposit #33

The Deposit #33 is situated in the eastern part of the Sredny Kraka. It is typical podiform and may be classified as subconcordant in the structural aspect (Saveliev, Kozhevnikov, 2015). The ore body contains massive chromitite surrounded by a thin (0.1–3 m) dunite envelope. The length of the ore body is 50 m. Its thickness is 1.5–2 m. There are numerous features of thinning up to pinching and thickening. Nodular chromitite appears occasionally in the boundary between massive chromitite and dunite. It was found that the olivine fabric of the surrounding dunite is typically deformational in origin (Saveliev, 2013). Chrome spinel composition varies significantly along the cross-section of the deposit and covers all the ophiolite spinels range. In the country and wall spinel peridotites, the spinel grains contain less Cr (20.59–43.05% Cr_2O_3) but more Al (26.77–45.55% Al_2O_3). The Cr-poorest spinels are found in the peridotite (СК-103-2L3) which is closest to the dunite. They have 52.34–54.87% Al_2O_3 and 12.56–15.3% Cr_2O_3. The Cr content of spinel grains increases in the dunite envelope (53.94–55.13% Cr_2O_3) and in the ore (60.8–62.2% Cr_2O_3).

Saksey deposit

Saksey-Klyuchevskaya area is situated in the southwestern part of Sredny Kraka and comprises several chromite-bearing zones. They are tabular-like dunite bodies, which run parallel to the mantle/crust boundary (paleo-Moho) and contain numerous small chromitite veins. A transition from harzburgite to dunite is usually gradational. There occur intermediate rocks containing a few pyroxene grains. There are three (Saksey, Klyuchevskoe and Shatran) deposits of disseminated chromitite in the area (Saveliev, Snachev, 2012).

The Saksey deposit comprises several small chromitite veins (2 to 5) within a thick dunite layer on the border between the mantle and crust sections. The sizes of the ore veins are as follows: the length is from n*10 m to 100 m, width is from several meters to n*10 m, and thickness is from several cm to 2 m. The chromitites strike varies from NNW 330° to NNE 10°. Their dip is almost vertical. The banded fine-grained ore is the most common in this deposit. There is an enclosed silicate structure too. It is presented by numerous scattered ovoid pieces of serpentinized olivine, with an average diameter of up to 2.5 cm and the length/width ratio ranging from 2 to 5, surrounded by chromite grains. The olivine maximum axis is usually oriented parallel to chromitite bands.

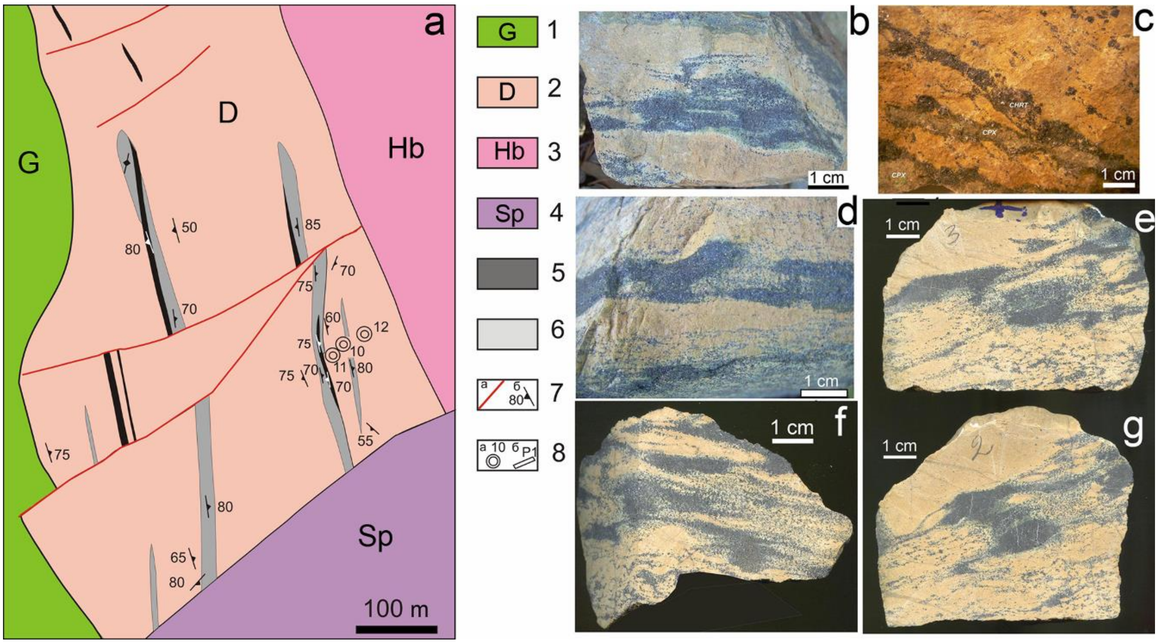

Fig. 3. *Schematic geological map of Saksey deposit (a) and structural features of chromitite (b–g): 1 – crust section (gabbro, clinopyroxenite, werlite with less serpentinite and metasomatic-altered gabbro), 2 –mainly dunite, 3 – spinel peridotite with less dunite, 4 – serpentinite, 5 – disseminated chrome ore, 6 – dunite with increased share of chromite, 7 – structural elements: a – faults, b – banding and aggregate lineation of chromite grains, 8 – bore holes (a) and trench (b); geological map after E.A. Shumikhin, V.V. Radchenko (1979)*

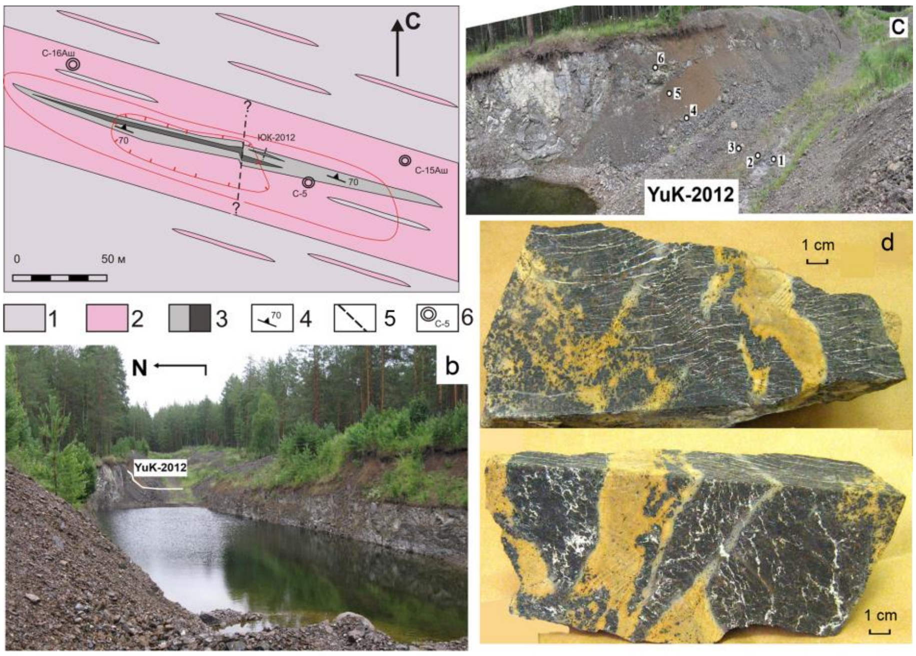

Fig. 4. *Schematic geological map of Pridorozhnoe deposit and structural features of chromitite: 1 – serpentinized peridotite, 2 – serpentinized dunite, 3 – disseminated chrome ore: a – rarely disseminated (10–20 % chromite grains), b – banded alternation of densely disseminated ore and dunite, 4 – foliation and banding in ultramafic rocks and chromitite, 5 – fault, 6 – boreholes*

Tiny clinopyroxenite veinlets crossing an ore banding at a sharp angle (10 to 30°) were found within the deposit. These veinlets may be single or numerous, forming a net. The chromitite bands occasionally show folding, thickening or nodes inclining at different angles towards the band direction (Fig. 3). There are dunite streams crossing the ore bands at different angles too. They were earlier described (Kravchenko, 1969; Thayer, 1964) as «intra-ore dunite dykes». Therefore, the observed relationships suggest the ore formation during an inhomogeneous solid plastic flow of dunite-chromitite assemblage (Saveliev, 2012, 2013a).

Chrome spinel composition was found to be almost constant in the dunite and chromitite. The chromium content is high (Cr# = 0.7–0.85) but the Mg/(Mg+Fe) ratio is decreased with respect to that of country peridotite to 0.5–0.6 (Saveliev et al., 2008). The Cr# of accessory peridotite spinels is lower (0.3–0.5).

Deposits of Apshak area

Apshak area is located in the western block of Yuzhny Kraka, to the north from the above-described Bolshoy Bashart and Menzhinsky deposits (Fig.1). In general, Laktybash and Pridorozhnoe deposits have similar characteristics with the described above.

The chrome ore is poorer, disseminated, and fine-grained, normally containing from 10 to 50% chromite. The host rocks are presented usually by a fully serpentinized dunite. The extent of chromitite-bearing zones varies from 100 to 200 m, the dunite thicknesses are 50-100 m (Laktybash) and 20–40 m (Pridorozhnoe). The thickness of ore-bearing zones reaches 10–15 m. They contain tiny chromitite streams (0.05–0.3 m) parallel to each other.

The general direction of foliation and ore banding strike is W-NW 270–300º, dipping to N-NE 0–30º at almost vertical angles. There are some veinlets and spots of peridotite in the ore-bearing dunite. The foliation, chromite banding and lineation in both dunite and peridotite are coherent to each other. The banding often forms small folding. There are nodes presented by a few massive ore lenses (Fig.4). This morphological feature is found to be the most extensive in the central part of the Pridorozhnoe deposit. Numerous massive chromitite lenses bended to form isoclinal folds with axial planes parallel to each other were described (Fig.4 d). The observed feature is an evidence of the mantle matter redistribution during the plastic flow.

We have studied compositional variations of chrome spinels across the peridotite-dunite-chromitite succession in both Laktybash and Pridorozhnoe deposits (Fig. 5, a, b). The chromium concentration changes, in general, gradationally and depends on the rock petrography in the deposits. The lowest Cr# value is found in the large peridotite lenses (0.45–0.5), and it increases a little (to 0.55) in the thinner ones. In dunite, the Cr# increases more substantially (to 0.65–0.7) and achieves the maximal value in the disseminated chromitite (up to 0.75). The Mg# = Mg/(Mg+Fe) ratio changes independently of the Cr#. In the ore vein, its values may be low as well as high. However, the peridotite spinel normally shows a higher Mg# than dunite. Titanium is found in the spinel grains only as impurity. TiO_2 concentration is up to 0.35% in the dunite spinels and only up to 0.25% in the peridotite spinels.

Multiscale initial dunite veinlets

The ophiolite chromitite mineralization is usually connected with dunite. Therefore, investigation of tiny dunite veinlets in the peridotite may give important information about the ore formation initial stage. We studied dunite streams in the Kraka ophiolite areas comparable with those described above.

The outcrop A-795 is situated 250 m to the north of the Laktybash deposit. It is presented by the banded serpentinized spinel peridotite that shows a well-defined foliation. In these peridotites, several tiny dunite bands and lenses were observed. They have a thickness ranging from 5 to 50 cm (Fig. 5 c). Accessory chrome spinels grade in composition from 0.3 Cr# in peridotite to 0.65 Cr# in dunite. In addition, there is a scale factor. The larger dunite lens, the higher compositional contrast between its chrome spinel and that of peridotite. In addition, it has been found that in the dunite spinels, TiO_2 value is elevated up to 0.5%, and the Mg# decreases to 0.55. In contrast, the peridotite spinels contain less than 0.3% TiO_2 and their Mg# increases to 0.7.

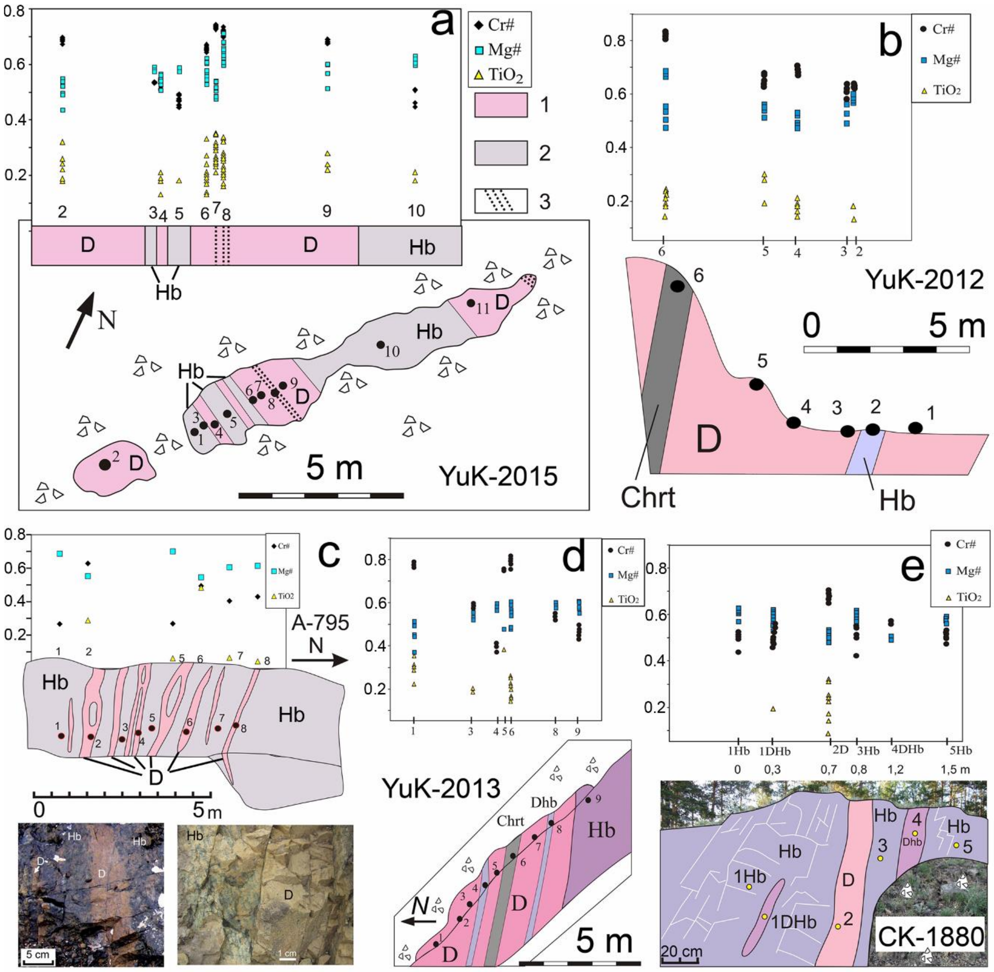

Fig. 5. *Compositional variation of chrome spinels along cross-sections of studied areas: a – Laktybash (YuK-2015), b – Pridorozhnoe (YuK-2012), c – outcrop A-795, d – outcrop YuK-2013, e – outcrop CK-1880. In Fig. 5 a: 1 – peridotite, 2 – dunite, 3 – disseminated chromite*

The outcrop YuK-2013 is situated 1 km east from the Laktybash and Pridorozhnoe deposits. This section is rather independent. Its matrix is a banded spinel peridotite with a changing pyroxene content (15 to 25%). The dunite body concordantly enclosed in the peridotite is 5m in thickness. The dunite contains several tiny disseminated chromitite streams (Fig. 5d). Across the peridotite-dunite-chromitite assemblage, spinel chemistry varies in a similar way to those described above. The lowest Cr# is found in the peridotite within dunite (0.4). It is quite higher in the host peridotite (0.5). A higher Cr# of chrome spinels was observed in dunite and the disseminated ore (0.6–0.85). Considerable content of TiO_2 is found only in the dunite and chromitite spinels (0.2–0.4%). The Mg# is quite constant along the cross-section (0.45–0.6).

The outcrop CK-1880 is located in the southern part of the Saksey-Klyuchevskaya area (Fig. 5 e). It is presented by banded peridotite. There is a broad range of pyroxene abundance in the rocks: 5 to 7% in dunite-harzburgite (sample CK-1880-1DHb), and 20 to 25% in Cpx-harzburgite (samples CK-1880-3, CK-1880-5). The lowest Cr# of spinel equal to 0.5 is found in peridotite. In the transitional rocks (CK-1880-1DHb and CK-

1880-4) its value is rather high, but variable. The dunite chrome spinels are characterized by the highest Cr# equal to 0.7. However, they contain only 0.1–0.35% of TiO_2. At the same sites, the lowest value of Mg# equal 0.5 was observed. It increased gradually to average 0.6 in peridotite.

The outcrop CK-103-2LB is situated 2 m east from the Deposit #33 chromitite orebody. Dunite veinlets, which are of several mm to 5cm in thickness, are found to be branching from the main dunite body and crossing a peridotite matrix having up to 30% of pyroxene grains. One of these veinlets was studied in detail by chemical and structural methods. The samples were investigated using the X-ray tomography (Saveliev, Kozhevnikov, 2015). Chrome spinel grains were segregated into the thinnest streams elongated parallel to each other. The grains make up about 3% of dunite sample volume. This is more than 2–3 times higher than their average concentration in peridotite.

Olivine grains from both peridotite and dunite show a developed dislocation fabric that is typical for mantle tectonites. By means of oxidized decoration after (Kohlstedt et al., 1976), we observed single dislocations, their walls, glide bands, cross-slip sites and blocks with different dislocations density (Fig. 6). We have investigated some of thin sections from the dunite veinlet on the universal stage (Fedorov Stage) and found that olivine grains have a strong crystallographic preferential orientation (CPO) indicating the rock origin under the high-T plastic flow condition. It has been revealed that olivine was deformed by a slip system {0kl}[100] (Saveliev, Blinov, 2015).

Numerous newly-formed spinel grains were observed in the polycrystalline olivine of the same sample. They vary in morphology and sizes. The thinnest acicular precipitates (only 0.3–0.5 μm thick and up to 10 μm long) are aligned in olivine grains along [010] axis (Fig. 7). A similar orientation of spinel needles was noted in (Franz, Wirth, 2000), where the study of ultramafic rock xenoliths from the Papua New Guinea basalt is presented. Bigger long irregular chrome spinel precipitations usually occur along grain and subgrain boundaries, and, occasionally, within grains themselves, along [100] axis (Saveliev, Blinov, 2015). There are often needle-like spinel branches from larger crystals ranging from 50 to 200 μm. Transitions from fine irregular precipitations of chrome spinels to bigger euhedral crystals are observed.

The studied spinels are characterized by the following composition features: the average Cr# =0.35, and Mg# = 0.51–0.68. The Cr# increases from peridotite – dunite contact (0.32) to dunite (0.39), whereas the Mg# decreases in the same direction. No significant regular variation of chemical composition is observed between the small and large grains.

Discussion

Numerous studies were conducted to explain chemical variations of accessory and ore-forming chrome spinels in the ophiolite and oceanic ultramafic rocks (Ahmed, 1984; Barnes, Roeder, 2001; Proenza et al., 1999). It was established that the ophiolite chrome spinel grains are characterized by a wide variation of Cr/Al ratio, a small difference in Mg/Fe ratio and low concentration of TiO_2 (Dickey, 1975; Leblanc, Violette, 1983; Thayer, 1964). Ophiolite ore-forming spinels were grouped into two types. The first is a high-Cr metallurgical type and the second is a high-Al refractory type (Hock et al., 1986; Perevozchikov et al., 2000; Prospecting…, 1987).

Most of the present models attempting to explain the podiform chromitite and host dunite origin are based on the assumption of a leading role of melts and fluids generated from the deeper mantle at the middle ocean ridges (MOR) and/or arc-related conditions (Ballhaus, 1998; Kubo, 2002; Roberts, 1988). Previous works assigned the primary importance to fractional crystallization and subsequent deformation (Dickey, 1975; Greenbaum, 1977; Hock et al., 1986; Thayer, 1964). Later on, almost all of the investigations were undertaken to find a pertinent condition for chrome spinel crystallization during different melts interaction, mixing or mingling (Ballhaus, 1998; Lago et al., 1982; Matveev, Ballhaus, 2002).

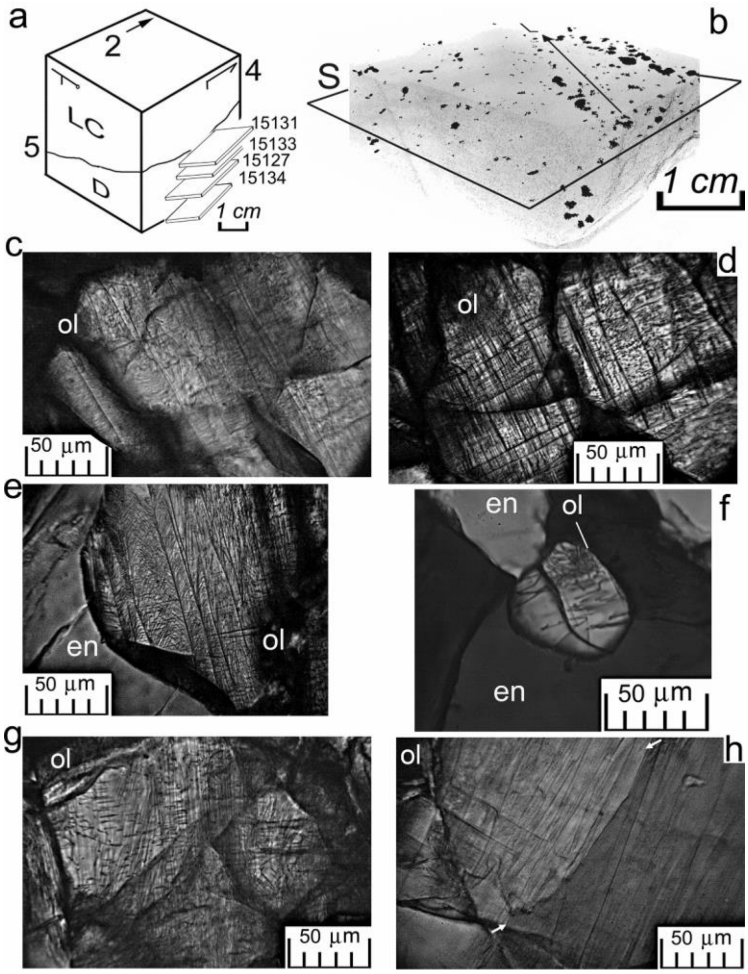

Fig. 6. *Framework of tiny dunite veinlet from peridotite (outcrop CK-103-2LB): a – 3D-outline of sample showing the location of dunite – peridotite contact and studied thin sections (on the cube planes – CK-103-2LB2, CK-103-2LB4, CK-103-2LB5; on the plane parallel to contact – 15127, 15131, 15133, 15134); b – X-ray view of the same dunite veinlet with chrome spinel grains after [51], S – banding, L – lineation, c - - photomicrographs of olivine dislocation structures obtained by oxygen decoration after [32], en –enstatite, and ol – olivine*

Most of the recent papers consider mantle-melt interaction in various tectonic settings as the main cause of the compositional variations of accessory and ore-forming spinels. They assume that high-Al spinels are formed beneath MOR, whereas high-Cr spinels appear in the supra-subduction zone (SSZ) condition. If the same peridotite block shows chrome ores of different spinel chemistry, they assume that it was repeatedly impregnated by melts in MOR-conditions earlier (producing high-Al spinel ore) and in SSZ-conditions later (producing high-Cr spinel ore) (Gonzalez-Jimenez et al., 2011; Morishita et al., 2006). If both high-Cr spinel ore and high-Al spinel are separated in the massif volume, they infer that these blocks were formed in a different setting and came into contact tectonically (Melcher et al., 1997).

However, to prove these points of view on the podiform chromitite origin (mantle – peridotite interaction, and magma mingling or mixing) it is necessary to answer numerous questions. Some of them are of the «how to explain» type: 1) presence of distinct boundaries along with gradational transitions between dunite and peridotite (for example, those at the Deposit #33), 2) formation of massive chromitite lenses within a relatively thin dunite envelope (Deposit #33), 3) presence of chromitite folding within dunite (for example, at the Saksey, Bolshoy Bashart and Pridorozhnoe deposits), and 4) presence of the pervasive deformation structures along with «previous magmatic» poikilitic inclusions of olivine in the chromite grains.

We suggest an alternative model of dunite and chromitite formation using the Kraka ophiolite as an example. Our hypothesis is based on empirical observations. It is well known that the ophiolite chromitite deposits show a wide variation of the 1) concentration of mineralization and 2) size of deposits. The first parameter may be called «intensive». It can be expressed quantitatively by the relative proportion of the massive and disseminated ores. The second parameter may be called «extensive» and it is equal to the ore resource. In addition, there is a well known similarity in the geological and mineralogical features of most ophiolite chromitite deposits all over the world. In particular, there is a symmetric sequence «wall peridotite – dunite envelope – chromitite body». Thus, a transition from small disseminated chromitite streams (initial stage) to a great massive chromitite deposit (terminal stage) is a result of the same ore-forming process which may be interrupted at any stage. Therefore, if the ore-forming process ended abruptly at early stages, the ore and surrounded rocks should retain numerous attributes of the acting mechanism.

For example, if it is suggested that chrome ore and dunite were formed by «melt - mantle interaction» (Arai, Miura, 2015; Gonzalez-Jimenez et al., 2014; Kelemen et al., 1992; 1995; Zhou et al., 2001), pyroxene grains retained from dissolution, along with considerable abundance of reaction products precipitated in the same place, should be present. In case of magma-mixing or magma-mingling models (Ballhaus, 1998; Matveev, Ballhaus, 2002), considerable amount of crystallized mafic-melts products (such as plagioclase and clinopyroxene) should occur within dunite and chromitite. However, there are only micro-inclusions in the chromite grains (McElduff, Stumpfl, 1991), and it does not clearly prove that the above assumptions are true.

The deposits and occurrences of Kraka ophiolite are typical objects where an ore-forming process was interrupted at different stages. Earlier stages are registered in the majority of occurrences of the Apshakskaya and Saksey-Klyuchevskaya areas where there is concordant disseminated chromitite. A more advanced stage is recorded in the Deposit #33 where we observe a typical podiform massive chromitite body. In numerous places, there are tiny dunite stringers in peridotite, embodying an initial stage of the ore-forming process.

On the studied sites, the ultramafic rocks show a developed deformation structure. As it was mentioned above, olivine grains have a strong fabric, indicating the rock origin under high-T plastic flow condition (Fig. 8). Our data are comparable to those obtained by experimental works (e.g. Carter, 1976; Chernyshov, 2001; Goncharenko, 1989; Poirier, 1988) and to those from other ophiolite ultramafic rocks (e.g. Chernyshov, Yurichev, 2013; Nicolas et al., 1971; Shcherbakov, 1990).

The plastic flow of polycrystalline olivine was accompanied by segregation of impurities that formed submicron exsolutions (Saveliev, Blinov, 2015), like those in metals (e.g. Novikov, 1986) . We have observed different stages of their formation. The first is the origin of needle-like exsolutions along [010] axes of olivine grains, then they form along subgrain and grain boundaries. Consistently, coalescence and spheroidization take place, resulting in the formation of typical euhedral chromite crystals in dunite. The X-ray tomography of the same samples shows the elongation of newly formed chrome spinel grains along the dunite – peridotite contact and foliation of olivine grains (Saveliev D.E., Kozhevnikov 2015). These observations support a relationship between the mantle solid flow and different mineral phases’ redistribution during the process.

Morphology of chrome spinel grains in the ophiolite ultramafic rocks is known to change regularly from skeletal and xenomorphic one in lherzolite and harzburgite to euhedral in dunite (e.g. Matsumoto, Arai, 2001). However, in the massive ore, the chromite grains are often anhedral (e.g. Thayer, 1964), and the formation of skeletal chromite was described in the nodular ore (Greenbaum, 1977; Leblanc, 1980; Prichard et al., 2015). The above-mentioned morphological changes are often accompanied by the Cr# increase of chrome spinels but it is not explained by magmatic and reaction models. Similar features were found in the studied places of Kraka. As shown in Fig. 9, the chrome spinel chemistry has some Cr# gap when considered on the ore-zone scale. Its location and size depend on the deposit type. A smaller gap occurs if the disseminated chromitites are considered. In contrast, a big compositional gap is found in case of the podiform massive ore deposits.

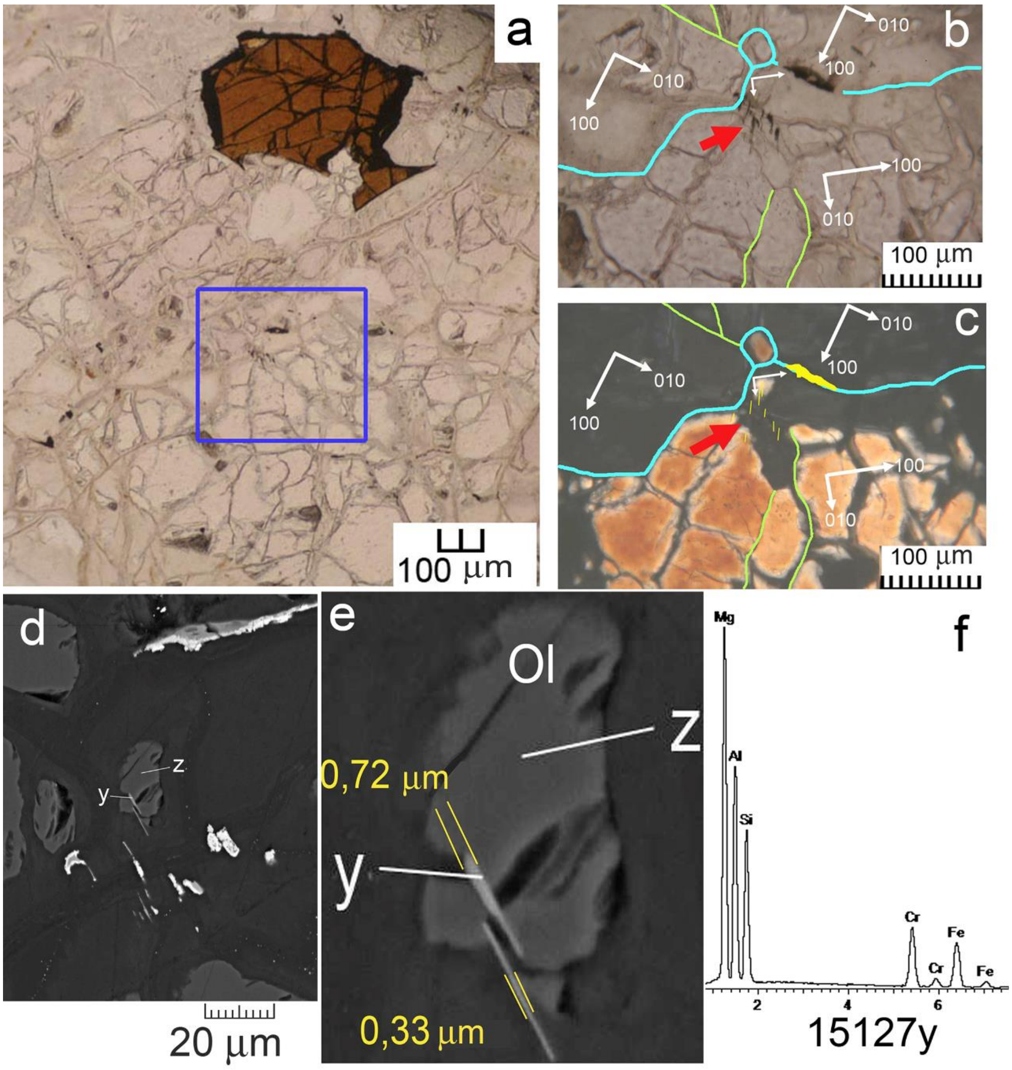

Fig. 7. *Needle-like exsolutions of chrome spinels in olivine grain volume (sample CK-103-2LB, thin section 15127); after [48]: a) – general view of thin section, the place contoured by dark-blue line is shown in b) (without analyzer) and c) (with analyzer), the arrow points to the site that is shown in detail in d); d) – (central part of b) and c)) – BSE-micrograph, black – serpentine, dark-grey – olivine, light-grey – chrome spinel, white – magnetite; e) – a more detailed image of d); f) – qualitative spectrum that supports identification of needle-like exsolutions as chrome spinels. In b) and c) grain and subgrain boundaries of olivine are painted by light lines. In c) the exsolutions of spinel are painted, arrows indicate the main directions in the olivine cell (arrow direction shows the rise of these axes)*

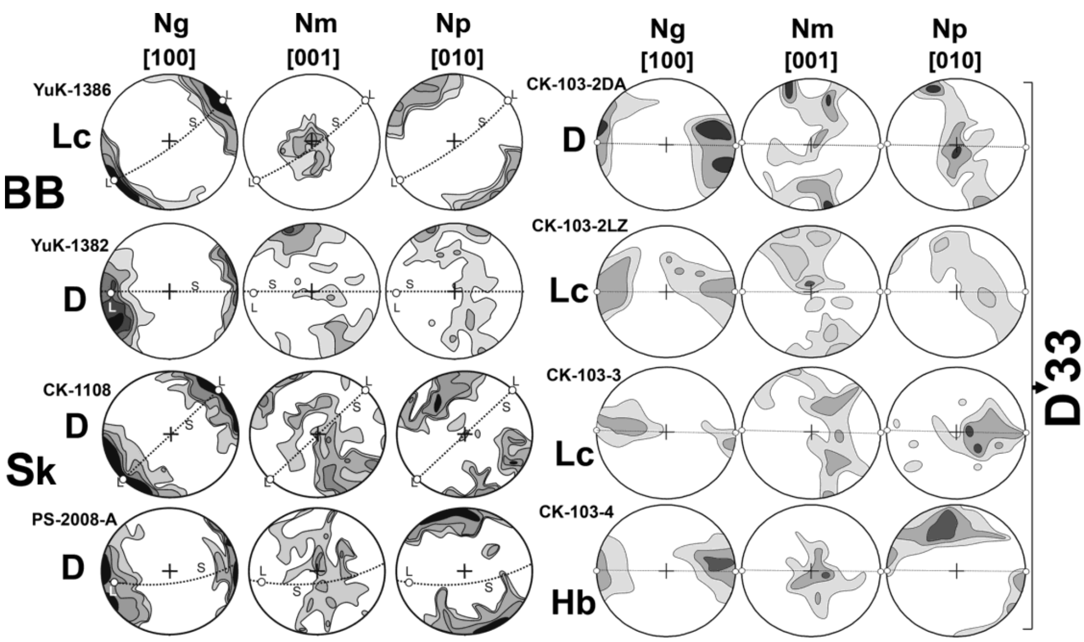

Fig. 8. *Crystallographic preferential orientation of olivine grains in the dunite from studied areas. Plots were made on the Wulf net, upper hemisphere, numbers of calculated points vary from 105 to 120; BB – Bolshoj Bashart, Sk – Saksey, D-33 – Deposit #33, S – foliation, L – lineation*

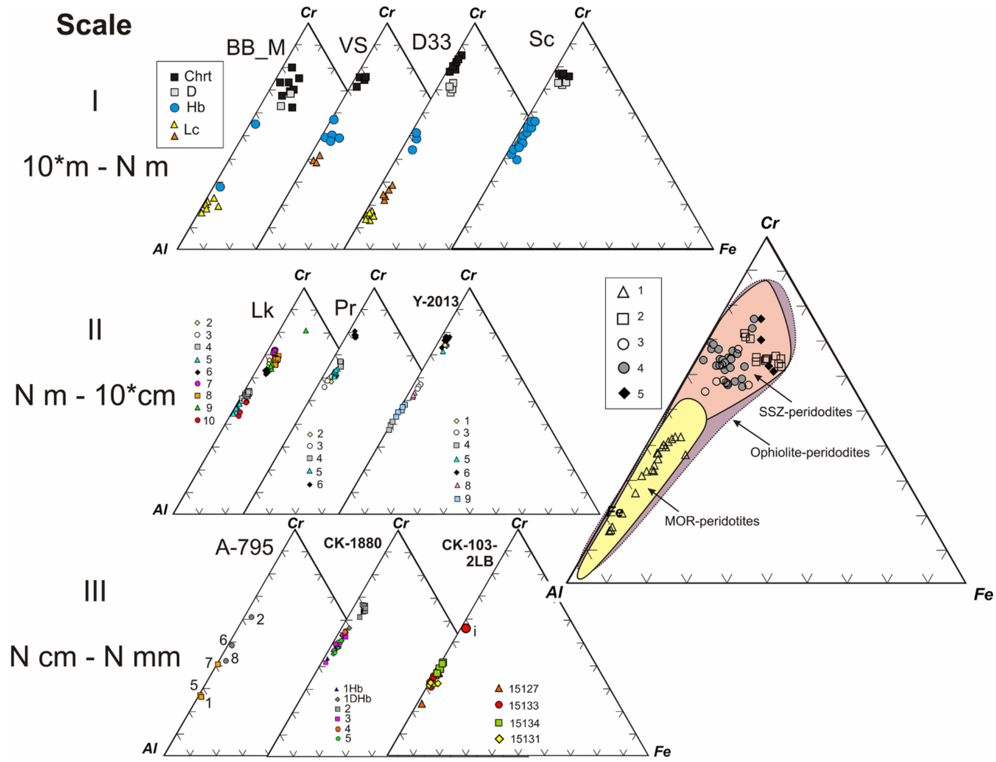

Fig. 9. *Compositional variations of chrome spinels in different areas of the Kraka massif in multiscale view. Scale I: Chrt – chromitite, D – dunite, Hb – harzburgite, Lc – lherzolite; Scale II: Lk, Pr, Y-2013 – point numbers correspond to the local sample numbers (Lk=YuK-2015), (Pr=YuK-2012), (Y-2013=YuK-2013); Scale III: point numbers correspond to the local sample numbers. For the general plot (on the right): 1 – peridotite, 2 – dunite-I from mantle section (paleo-Moho), 3 – dunite-II close to the crust-mantle boundary, 4 – chromitites in dunite-I, 5 – chromitites in dunite-II; colored areas show chemical variations of spinel grains from peridotites from ophiolites, middle oceanic ridges (MOR) and supra subduction zones (SSZ)*

However, the gap of spinel chemistry does not occur in the peridotite impregnated by tiny dunite veinlets, and the Cr# changes gradually. In this case, we observed a presence of spinel skeletal forms similar to those in peridotite. Apparently, these forms were quickly disappearing due to the subsequent coalescence and spheroidization. As a result, the chrome spinel grains become more euhedral in form. During growth, these grains may enclose a part of olivine matrix, which leads to the formation of the olivine inclusion in the chromite grains that are non-magmatic in origin (Fig. 10). This phenomenon is well known for metallic systems.

Although spinel composition changes quite gradationally during their morphological transition, it may sometimes change quite sharply in places. In particular, in the thin sections 15127 and 15134, two points were found to have much lower Cr# compared to a general increase of this value. Both cases represent the needle-like chrome spinel exsolutions along the olivine grain boundaries. The point 15127s belongs to a needle-like branch (2-2.5 μm thick) from a bigger elongated grain 30x100 μm in size. In the remaining part of the grain volume, the Cr# is typical compared to that of the completely thin section. Similarly, the point 15127d gave a lower Cr#=0.32 in the thin needle-branch against the isometric grain, 70x70 μm in dimension.

Besides, we found a sharp increase of the spinel Cr# in the same grains from the thin section 15133 where stress was shown (points 15133 i, k). In both cases, the increase of Cr# and, accordingly, the decrease of Mg# were found in the places where the grains were thinned and they were enclosed in the olivine grains of a comparable size (Fig. 10 e, f). At the same time, chemistry of the rest grains is similar to that in the whole volume of the sample.

As shown above, the accessory and ore-forming chrome spinel composition changes at the transition from the initial stage to more advanced stages on different scales of the observation. We have also pointed out the relationship between the chemical and structural features of the ore-bearing zones. Therefore, we believe that all marked attributes of the Kraka dunite and chromitite may be well explained only by a rheomorphic model that suggests cooperative changes of both ultramafic rocks structure and chemistry during their solid flow.

The main trigger of impurity segregation and coalescence in the olivine grain could be plastic deformation that is accompanied by mantle upwelling in the decompression zones. The rise to the less dense levels of lithosphere was accompanied by a decrease of the olivine cell capacity for impurities, in particular, chromium and aluminum. On the other hand, they were an obstacle for dislocations movement in the olivine grains, which promoted their blocking and polygonization. The exsolutions of the harder phase, such as spinel, formed much strain around themselves due to a decrease of the solid flow speed. Because of these processes, two mineral phases were redistributed in space.

Spheroidization is a final stage of exsolutions arrangement into the euhedral chrome spinel crystals that are typical for the ophiolitic dunite. This process is shown in a tendency to take their crystallographic habitus. A driving force of spheroidization is the grain boundary free energy minimization, as this was understood in metals many years ago (e.g. Novikov, 1986).

The thermodynamic basis of mineral phases' redistribution in the mantle solid flow was given by (Fedoseev, 2016; Saveliev, Fedoseev, 2011; 2014). It is suggested that the localization of plastic flow in the weakest layers should occur during decompression accompanying ascending of the mantle. Since olivine is the softest mineral of the mantle, as shown in (Carter, 1976; Saveliev, Fedoseev, 2011; Yamamoto et al., 2008), a solid flow should be faster in dunite than in peridotite. Therefore, the mineral phase redistribution in dunite is more efficient too. Chromite could be brought into dunite in two ways.

First, as mentioned above, it could be the deformation-induced impurities segregation from olivine grains.

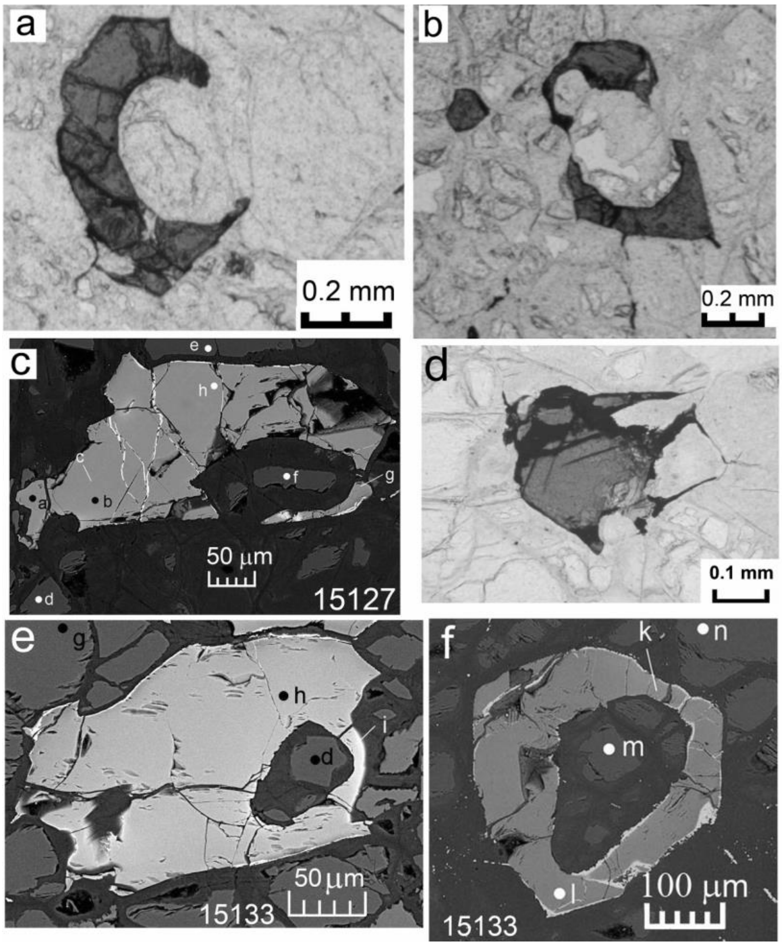

Fig.10. *Different stages of the solid deformation induced formation of olivine inclusions in the chrome spinel grains (sample CK-103-2LB): a, b, d – photomicrographs in the plane polarized transmission light, dark – chrome spinel, light – serpentinized olivine, c, e, f – BSE-images, light – chrome spinel, dark-grey - olivine, black – serpentine*

Second, it could be a deformation-induced breakdown of pyroxene grains because they are more brittle than olivine. Therefore, during the flow they could be reduced and dissolved. Under stress, the chrome spinel grains composition could be changed from high-Al to high-Cr. For all these above-mentioned processes, the critical zone is the narrow contact between dunite and peridotite where only we can see numerous newly-formed chrome spinel exsolutions.

Conclusion

The Kraka chromitite occurences and deposits consist of the high-C# chrome spinel grains (Cr# is more than 0.7). On scale of deposits and ore-bearing zones, the compositional contrast of chrome spinels is observed between peridotite, on the one hand, and dunite and chromitite, on the other. The noted chemical gap increases from disseminated ore deposits («dissipated mineralization») to typical podiform ones («concentrated mineralization»).

The structural and chemical investigation of thin initial dunite venlets in peridotite has shown that chrome spinel chemistry changes in them gradually and there is no Cr# gap between peridotite and dunite. It has been determined that the Cr# increases gradually from peridotite into the dunite veinlet. There are quite sharper changes in stressed places.

Within dunite veinlets, numerous newly formed chrome spinel exsolutions were discovered. The thinnest acicular precipitates (only 0.3–0.5 μm thick) are aligned in olivine grains along [010] axis. Bigger long irregular chrome spinel precipitates usually occur along grain and subgrain boundaries and occasionally within grains themselves, along [100] axis. Changes from the fine irregular precipitates of chrome spinels to bigger euhedral crystals are observed. During growth, these grains may occupy part of olivine matrix, which leads to the formation of olivine inclusions in the chromite grains that are non-magmatic in origin. By analogy with dynamic aging (dispersion hardening) in metals, the noted structural and chemical alterations in dunites are interpreted as deformation-induced segregation of impurities.

Futher on, the inhomogenous plastic flow was driving the mineral phases redistribution that has formed dunite bodies as «more mobile matter» in which the chromitite bodies were built. The leading role of solid plastic flow is supported by strong deformation fabric of olivine in all studied samples and by structural deformation features of them on different scales.

Acknowledgements. We are grateful to Professor Victor N. Puchkov who helped us arrange the manuscript in English. This work was performed as part of the government contract of The Federal Agency for Scientific Organizations (FASO Russia), theme «The model of chrome ore deposits formation in ophiolites» and project of The Russian Foundation for Basic Research (RFBR) № 14-05-97001.

References

Ahmed Z. 1984. Stratigraphic and textural variations in the chromite composition of the ophiolitic Sakhakot-Qila Complex, Pakistan. Economic Geology and Bull. Soc. Econ. Geologists. 79:1334-1359.

Arai S., Miura M. 2015. Podiform chromitites do form beneath mid-ocean ridges. Lithos. 232:143–149. doi:10.1016/j.lithos.2015.06.015

Ballhaus C. 1998. Origin of the podiform chromite deposits by magma mingling. Earth and Planetary Science Letters. 156:185-193. doi:10.1016/S0012-821X(98)00005-3

Barnes S., Roeder P. 2001. The Range of spinel compositions in terrestrial mafic and ultramafic rocks. Journal of Petrology. 42:2279-2302. doi:10.1093/petrology/42.12.2279

Carter N.L. 1976. Steady state flow of rocks. Rev. Geophys. and Space Phys. 14:301-360. doi:10.1029/RG014i003p00301

Cassard D., Nicolas A., Rabinowitch M., Moutte J., Leblanc M., Prinzhoffer A. 1981. Structural Classification of Chromite Pods in Southern New Caledonia. Economic Geology.76:805-831.

Chashchukhin I.S., Votyakov S.L., Shchapova Yu.V. 2007. Kristallokhimiya khromshpineli i oksitermobarometriya ultramafitov skladchatykh oblastey [Crystal chemistry of chrome spinel and oxithermobarometry of ultramafites of fold belts]. IG&G UrO RAN. Yekaterinburg, p. 310. (in Russian)

Chernyshov A.I. 2001. Ultramafity (plasticheskoe techenie, strukturnaya i petrostrukturnaya neodnorodnost) [Ultramafites (plastic flow, structural and petrostructural heterogeneity)]. Charodey, Tomsk, p.215. (in Russian)

Chernyshov A.I., Yurichev A.N. 2013. Petrostrukturnaya evolyutsiya ultramafitov Kalninskogo khromitonosnogo massiva v Zapadnom Sayane [Petrostructural evolution of ultramafic rock of the Kalninskiy chromite-bearing massif in the West Sayan]. Geotektonika, 4:31-46 (in Russian)

Denisova E.A. 1990. Stroenie i deformatsionnye struktury ofiolitovykh massivov s lertsolitovym tipom razreza [Framework Structure and deformation features of ophiolite with lherzolite type of section]. Geotektonika. 2:14-27. (in Russian)

Dick H.J.B., Bullen T. 1984. Chromian spinel as a petrogenetic indicator in abyssal and Alpine-type peridotites and spatially associated lavas. Contrib Mineral Petrol. 86:54-76. doi:10.1007/BF00373711

Dickey J.S. 1975. A hypothesis of origin for podiform chromite deposits. Geochim. et Cosmochim. Acta. 39:1061-1075. doi: 10.1016/0016-7037(75)90047-2

Fedoseev V.B. 2016. Stratification of two-phase monodisperse system in a laminar planar flow. Journal of Experimental and Theoretical Physics. 149(4):1-11.

Franz L., Wirth R. 2000. Spinel inclusions in olivine of peridotite xenoliths from TUBAF seamount (Bismarck Archipelago/Papua New Guinea): evidence for the thermalandtectonic evolution of the oceaniclithosphere. Contrib. Mineral. Petrol. 140:283-295. doi: 10.1007/s004100000188

Goncharenko A.I. 1989. Deformatsiya i petrostrukturnaya evolyutsiya alpinotipnykh giperbazitov [Deformation and petro structural evolution of alpinotype ultrabasites]. Tomsk

University Publishing. Tomsk, p. 404. (in Russian)

Gonzalez-Jimenez J.M., Griffin W.L., Proenza A., Gervilla F., O'Reilly S.Y., Akbulut M., Pearson N.J., Arai S. 2014. Chromitites in ophiolites: how, where, when, why? Part II. The crystallisation of chromitites. Lithos. 189:148–158. doi:10.1016/j.lithos.2013.09.008

Gonzalez-Jimenez J.M., Proenza J.A., Gervilla F., Melgarejo J.C., Blanco-Moreno J.A., Ruiz-Sanchez R., Griffin W.L. 2011. High-Cr and high-Al chromitites from the Sagua de Tanamo district, Mayari-Cristal ophiolitic massif (eastern Cuba): Constrains on their origin from mineralogy and geochemistry of chromian spinel and platinum-group-elements. Lithos. 125:101-121. doi: 10.1016/j.lithos.2011.01.016

Greenbaum D. 1977. The chromitiferous rocks of the Troodos ophiolite complex, Cyprus. Economic Geology. 72:1175-1194. doi: 10.2113/gsecongeo.72.7.1175

Hock M., Friedrich G., Plueger W.L., Wichowski A. 1986. Refractory- and metallurgical-type chromite ores, Zambales Ophiolite, Luzon, Philippines. Mineralium Deposita. 21:190-199. doi: 10.1007/BF00199799

Irvine T.N. 1965. Chromian spinel as a petrogenetic indicator. Part I: Theory. Canadian Journal Earth Science. 2:648-672. doi: 10.1139/e65-046

Kazantseva T.T., Kamaletdinov M.A. 1969. Ob allokhtonnom zaleganii giperbazitovykh massivov zapadnogo sklona Yuzhnogo Urala [About an allochtonous position of ultrabasic massifs of western slope of the Southern Urals]. Doklady AN USSR. 189:1077-1080. (in Russian)

Kelemen P.B., Dick H.J.B., Quick J.E. 1992. Formation of harzburgite by pervasive melt/rock reaction in the upper mantle. Nature. 358:635-641. doi: 10.1038/358635a0

Kelemen P.B., Shimizu N., Salters V.J.M. 1995. Extraction of mid-ocean-ridge basalt from the upwelling mantle by focused flow of melt in dunite channels. Nature. 375:747-753. doi:10.1038/375747a0

Kohlstedt D.L., Goetze C., Durham W.B., Sande van der J.B. 1976. A new technique for decorating dislocations in olivine. Science.191:1045-1046. doi:10.1126/science.191.4231.1045

Kravchenko G.G. 1969. Rol tektoniki pri kristallizatsii khromitovykh rud Kempirsayskogo plutona [Role of tectonics in crystallization of chromite ore of the Kempirsayskiy Pluton]. Moskva, Nauka, p.232. (in Russian)

Kubo K. 2002. Dunite formation processes in highly depleted peridotite: case study of the Iwanaidake Peridotite, Hokkaido, Japan. Journal of Petrology. 43:423-448. doi: 10.1093/petrology/43.3.423

Lago B.L., Rabinowicz M., Nicolas A. 1982. Podiform chromite ore bodies: a genetic model. Journal of Petrology. 23:103-125. doi: 10.1093/petrology/23.1.103

Leblanc M. 1980. Chromite Growth, Dissolution and Deformation from a Morphological View Point: SEM Investigations. Mineralium Deposita (Berl.). 15:201-210. doi: 10.1007/BF00206514

Leblanc M., Violette, J.-F. 1983. Distribution of aluminium-rich and chromium-rich chromite pods in ophiolite peridotites. Economic Geology.78:293-301. doi:10.2113/gsecongeo.78.2.293

Matsumoto I., Arai S. 2001. Morphological and chemical variations of chromian spinel in dunite-harzburgite complexes from the Sangun zone (SW Japan): implications for mantle/melt reaction and chromitite formation processes. Mineralogy and Petrology. 73:305-323. doi:10.1007/s007100170004

Matveev S., Ballhaus C. 2002. Role of water in the origin of podiform chromitite deposits. Earth and Planetary Science Letters. 203:235-243. doi: 10.1016/S0012-821X(02)00860-9

McElduff B., Stumpfl E.F. 1991. The chromite deposits of the Troodos complex, Cyprus - evidence for the role of a fluid phase accompanying chromite formation. Mineralium Deposita. 26:307-318. doi: 10.1007/BF00191079

Melcher F., Grum W., Simon G., Thalhammer T.V., Stumpfl E.F. 1997. Petrogenesis of the ophiolitic giant chromite deposits of Kempirsai, Kazakhstan: a study of solid and fluid inclusions in chromite. Journal of Petrology. 38:1419-1458.

Morishita T., Andal E.S., Arai S., Ishida Y. 2006. Podiform chromitites in the lherzolite-dominant mantle section of the Isabela ophiolite, the Philippines. Island Arc. 15:84-101. doi: 10.1111/j.1440-1738.2006.00511.x

Nicolas A., Bouchez J.L., Boudier F., Mercier J.C. 1971. Textures, structures and fabrics due to solid state flow in some European lherzolites. Tectonophysics. 12:55-86. doi: 10.1016/0040-1951(71)90066-7

Novikov I.I. 1986. Teoriya termicheskoy obrabotki metallov [Theory of thermal processing of metals]. Moskow, Metallurgiya, p. 480. (in Russian)

Pavlov N.V., Kravchenko G.G., Grigoryeva-Chuprynina I.I. 1968. Khromity Kempirsayskogo plutona [Chromitites of the Kempirsay Pluton]. Moskow, Nauka, p. 178. (in Russian)

Perevozchikov B.V. 1995. Zakonomernosti lokalizatsii khromitovogo orudeneniya v alpinotipnykh giperbazitakh [Features of chrome ore localization in the alpine-type ultrabasics]. Geoinformmark. Moskow. (in Russian)

Perevozchikov B.V., Bulykin L.D., Popov I.I. et al. 2000. Reestr khromitovykh mestorozhdeniy v alpinotipnykh giperbazitakh Urala [The nomenclature of chromite deosits in alpinotype ultrabasics of the Urals]. Perm, KamNIIKIGS, p. 474. (in Russian)

Poirier J.-P. 1985. Creep of crystals. High-temperature deformation processes in metals, ceramics and minerals. London, Cambridge University Press.

Poiski, razvedka i otsenka khromitovykh mestorozhdeniy [Prospecting, exploration and economic evaluation of chrome ore deposits]. *Eds*. Smirnova T.A., Segalovich V.I. 1987. Moscow. Nedra. (in Russian)

Prichard H.M., Barnes S.J., Godel B., Reddy S.M., Vukmanovic Z., Halfpenny A., Neary C.R., Fisher P.C. 2015. The structure of and origin of nodular chromite from the Troodos ophiolite, Cyprus, revealed using high-resolution X-ray computed tomography and electron backscatter diffraction. Lithos. 218–219:87–98. doi:10.1016/j.lithos.2015.01.013

Proenza J., Gervilla F., Malgarejo J.C., Bodinier J.L. 1999. Al- and Cr-rich chromitites from the Mayari-Baracoa ophiolite Belt (Eastern Cuba): consequence of interaction between volatile-rich melts and peridotites in suprasubduction mantle. Economic Geology. 94:547-566. doi:10.2113/gsecongeo.94.4.547

Roberts S. 1988. Ophiolitic chromite formation: a marginal basin phenomenon? Economic Geology. 83:1034-1036. doi: 10.2113/ gsecongeo.83.5.1034

Saveliev D.E. 2012. Khromitonosnost giperbazitovykh massivov Yuzhnogo Urala [Chromite content of ultrabasic massifs of the Southern Urals. Diss. Dr. Geol.-Min. Sci., Perm State University. (in Russian)

Saveliev D.E. 2013a. Proiskhozhdenie nodulyarnykh tekstur (na primere khromitov vostochnoy chasti massiva Sredniy Kraka, Yuzhnyy Ural) [Origin of nodular texture (example of chromite from the eastern part of Sredniy Kraka massif, Southern Urals). Rudy i metally. 5:41-49 (in Russian)

Saveliev D.E. 2013b. Sootnoshenie struktur rudonosnoy dunit-khromitovoy assotsiatsii I peridotitov v ofiolitakh (na primere massivov Kraka) [Relationship between the structures of ore-bearing dunite-chromitite association and peridotites in the ophiolites (on the example of Kraka massifs). Litosfera. 2:76- 91 (in Russian)

Saveliev D.E., Blinov I.A. 2015. Sindeformatsionnye vydeleniya khromshpinelidov v plasticheski deformirovannykh agregatakh olivina (ofiolity Kraka, Yuzhnyy Ural) [Syndeformation chrome spinel inclutions in the plastically deformed olivine aggregates (Kraka ophiolite, the Southern Urals)]. Vestnik Permskogo Universiteta. Geologiya, 4(29):45-69. doi: 10.17072/psu.geol.29.44 (in Russian)

Saveliev D.E., Fedoseev V.B. 2011. Segregatsionnyy mekhanizm formirovaniya tel khromitov v ultrabazitakh skladchatykh poyasov [Segregation mechanism of chromitite body formation in the ultrabasic rocks of fold belts]. Rudy i metally. 5:35-42. (in Russian)

Saveliev D.E , Fedoseev V.B. 2014. Plasticheskoe techenie i reomorficheskaya differentstatsiya veshchestva v mantiynykh ultramafitakh [Plastic flow and rheomorphic differentiation of the mantle ultramaflc rocks]. Vestnik Permskogo universiteta. Geologiya. 4(25):22-41. doi:10.17072/psu.geol.25.22. (in Russian)

Saveliev D.E., Kozhevnikov D.A. 2015. Strukturnye i petrograficheskie osobennosti ultramafitov na uchastke mestorozhdeniya #33 v vostochnoy chasti massiva Sredniy Kraka (Yuzhnyy Ural) [Textural and Petrographic Features of Ultramaflc Rocks within Area of "Deposit #33", Eastern Part of Sredniy Kraka Massif (South Urals)]. Vestnik Permskogo Universiteta. Geologiya. l(26):60-84. doi:10.17072/psu.geol.26.60 (in Russian)

Saveliev D.E., Snachev V.I. 2012. Bednovkraplennye khromovye rudy Yuzhnogo Urala i perspektivy ikh prakticheskogo ispolzovaniya [Deposits of poor chromite-ores of the South Urals and prospects of their use]. Rudy i metally. 2:36-40. (in Russian)

Saveliev D.E., Belogub E.V., Kotlyarov V.A. 2014. Mineralogo-geokhimicheskaya zonalnost i deformatsionnyy mekhanizm formirovaniya khromitit-dunitovykh tel v ofiolitakh (na primere massiva Kraka, Yuzhnyy Ural) [Mineral-geochemical zonation and deformation mechanism of formation of chromitite- dunite bodies in ophiolites (on the example of Kraka massif, South Urals)]. *In* Metallogeniya drevnikh i sovremennykh okeanov - 2014. IMin UrO RAN, Miass, pp. 95-98 (in Russian)

Saveliev D.E., Snachev V.I., Savelieva E.N., Bazhin E.A. 2008. Geologiya, petrogeokhimiya i khromitonosnost gabbro-giperbazitovykh massivov Yuzhnogo Urala [Geology, petrogeochemistry, and chromite content of gabbro - ultrabasic massifs of the South Urals]. Ufa, DizaynPoligrafServis. p. 320. (in Russian)

Savelieva G.N. 1987. Gabbro-ultrabazitovye kompleksy ofiolitov Urala i ikh analogi v sovremennoy okeanicheskoy kore [Gabbro-ultrabasic complexes of the Urals ophiolites and their analogues in the present-day oceanic crust]. Nauka. Moscow, p. 230. (in Russian)

Senchenko G.S. 1976. Skladchatye struktury Yuzhnogo Urala [The folding structures of the Southern Urals]. Nauka. Moscow, p. 172. (in Russian)

Shcherbakov S.A. 1990. Plasticheskie deformatsii ultrabazitov ofiolitovoy assotsiatsii Urala [Plastic deformations of ultrabasic rock of the Urals ophiolite association]. Moscow. Nauka, p. 120. (in Russian)

Snachev V.I., Saveliev D.E., Rykus M.V. 2001. Petrogeokhimicheskie osobennosti porod i rud gabbro-giperbazitovykh massivov Kraka [Petrogeochemical features of rocks and ores of gabbro-ultrabasic Kraka massifs]. BashGU. Ufa, p. 212. (in Russian)

Thayer T.P. 1964. Principal features and origin of podiform chromite deposits, and some observations on the Guleman-Soridag District, Turkey. Economic Geology. 59:1497-1524. doi:10.2113/gsecongeo.59.8.1497

Yamamoto J., Ando J., Kagi H., Inoue T., Yamada A., Yamazaki D., Irifune T. 2008. In situ strength measurements on natural upper-mantle minerals. Phys. Chem. Minerals. 35:249–257. doi:10.1007/s00269-008-0218-6

Zhou M.-F., Malpas J., Robinson P.T., Sun M., Li J.-W. 2001. Crystallization of podiform chromitites from silicate magmas and the formation of nodular textures. Resource Geology. 51:1-6. doi:10.1111/j.1751-3928.2001.tb00076.x

Zhou M.-F., Robinson P. 1994. High-Cr and high-Al podiform chromitites, western China: Relationship to partial melting and melt/rock reaction in the upper mantle. International Geology Review. 36:678 – 686. doi:10.1080/00206819409465481

Вариации состава хромшпинелидов в рудоносных зонах офиолита Крака и происхождение хромититов

Д.Е.Савельев[a], И.А. Блинов[b]

[a]Институт геологии УНЦ РАН, 450077, Уфа, ул.К.Маркса, 16/2
E-mail: savl71@mail.ru

[b]Институт минералогии УрО РАН, 456301, Челябинская область, Миасс, Ильменский заповедник. E-mail: ivan_a_blinov@mail.ru

Рассмотрены вариации состава акцессорных и рудообразующих хромшпинелидов в ультрамафитах Крака, начиная от масштаба месторождений и заканчивая масштабом шлифов, взаимосвязи особенностей состава и структуры в породах и рудах. На всех изученных участках ультрамафиты и хромититы обнаруживают деформационную структуру и развитые текстуры деформации оливина. В масштабе рудных зон постоянно наблюдается определенный разрыв в величине отношения Cr#=Cr/(Cr+Al) между перидотитами и хромититами, с одной стороны, и перидотитами, околорудными дунитами – с другой. Положение этого разрыва на диаграмме изменяется в зависимости от типа месторождения, увеличиваясь от табулярных тел, сложенных вкрапленными рудами, к типично подиформным массивным хромитам. Исследованы тонкие инициальные дунитовые прожилки в перидотитах и показано, что состав хромшпинелидов при их формировании изменяется постепенно и разрыв состава по Cr# между перидотитами и дунитами не имеет места. Дунитовые прожилки показывают четкую предпочтительную кристаллографическую ориентировку оливина, свидетельствующую о формировании их в условиях высокотемпературного пластического течения. В прожилках зафиксированы различные стадии роста новообразованных зерен хромшпинелидов, обусловленные сегрегацией примесей, коалесценцией и сфероидизацией в ходе пластического течения поликристаллического оливинового матрикса. Делается вывод о ведущей роли твердофазного течения в перераспределении главных мантийных минералов – оливина и пироксенов, которое приводит к обособлению наиболее мобильных дунитовых тел, а внутри них – к сегрегации примесных элементов в виде хромитовой минерализации. Обсуждается роль пластической деформации в инициации частичного плавления перидотитов и образовании новых зерен хромшпинелидов.

Ключевые слова: *хромшпинелиды, офиолиты, ультрамафиты, пластическое течение, подиформные хромититы*.

Библиографический список

Гончаренко А.И. Деформация и петроструктурная эволюция альпинотипных гипербазитов. Томск: Изд-во Томского ун-та, 1989. 404 с.

Денисова Е.А. Строение и деформационные структуры офиолитовых массивов с лерцолитовым типом разреза // Геотектоника. 1990. № 2. С. 14-27.

Казанцева Т.Т., Камалетдинов М.А. Об аллохтонном залегании гипербазитовых массивов западного склона Ю. Урала // Докл. АН СССР. 1969. Т. 189, № 5. С. 1077-1080.

Кравченко Г.Г. Роль тектоники при кристаллизации хромитовых руд Кемпирсайского плутона. М.: Наука, 1969. 232 с.

Новиков И.И. Теория термической обработки металлов. М.: Металлургия, 1986. 480 с.

Павлов Н.В., Кравченко Г.Г., Чупрынина И.И. Хромиты Кемпирсайского плутона. М.: Наука, 1968. 178 с.

Перевозчиков Б.В. Закономерности локализации хромитового оруденения в альпинотипных гипербазитах. М.: Геоинформмарк, 1995. 47 с.

Пуарье Ж.С.П. Ползучесть кристаллов. Механизмы деформации металлов, керамики и минералов при высоких температурах. М.: Мир, 1988. 287 с.

Поиски, разведка и оценка хромитовых месторождений/ под ред. Т.А.Смирновой, В.И.Сегаловича. М.: Недра, 1987. 166 с.

Реестр хромитовых месторождений в альпинотипных гипербазитах Урала / под ред. Б.В.Перевозчикова. Пермь, 2000. 474 с.

Савельев Д.Е. Хромитоносность гипербазитовых массивов Южного Урала: дис. … д-ра геол.-мин. наук. Уфа, 2012. 410 с.

Савельев Д.Е. Происхождение нодулярных текстур (на примере хромититов восточной части массива Средний Крака, Южный Урал) // Руды и металлы. 2013. №5. С. 41-49.

Савельев Д.Е. Соотношение структур рудоносной дунит-хромититовой ассоциации и перидотитов в офиолитах (на примере массивов Крака) // Литосфера. 2013. №2. С.76-91.

Савельев Д.Е., Блинов И.А. Синдеформационные выделения хромшпинелидов в пластически деформированных агрегатах оливина (офиолиты Крака, Южный Урал) // Вестник Пермского университета. Геология. 2015. №4 (29). С. 44-69.

Савельев Д.Е., Федосеев В.Б. Сегрегационный механизм формирования тел хромититов в ультрабазитах складчатых поясов // Руды и металлы. 2011. №5. С. 35-42.

Савельев Д.Е., Федосеев В.Б. Пластическое течение и реоморфическая дифференциация вещества в мантийных ультрамафитах // Вестник Пермского университета. Геология. 2014. №4 (25). С. 22-41.

Савельев Д.Е., Кожевников Д.А. Структурные и петрографические особенности ультрамафитов на участке «месторождение

№33» в восточной части массива Средний Крака (Южный Урал) // Вестник Пермского университета. Геология. 2015. №1 (26). С. 60-84.

Савельев Д.Е., Сначев В.И. Бедновкрапленные хромовые руды Южного Урала и перспективы их практического использования // Руды и металлы. 2012. № 2. С. 36-40.

Савельев Д.Е., Белогуб Е.В., Котляров В.А. Минералого-геохимическая зональность и деформационный механизм формирования хромитит-дунитовых тел в офиолитах (на примере массива Крака, Южный Урал) // Металлогения древних и современных океанов-2014. Двадцать лет на передовых рубежах геологии месторождений полезных ископаемых. Имин УрО РАН. Миасс, 2014. С. 95-98.

Савельев Д.Е., Сначев В.И., Савельева Е.Н., Бажин Е.А. Геология, петрогеохимия и хромитоносность габбро-гипербазитовых массивов Южного Урала. Уфа: ДизайнПолиграфСервис, 2008. 320 с.

Савельева Г.Н. Габбро-ультрабазитовые комплексы офиолитов Урала и их аналоги в современной океанической коре. М.: Наука, 1987. 230 с.

Сенченко Г.С. Складчатые структуры Южного Урала. М.: Наука, 1976. 172 с.

Сначёв В.И., Савельев Д.Е., Рыкус М.В. Петрогеохимические особенности пород и руд габбро-гипербазитовых массивов Крака / БашГУ. Уфа, 2001. 212 с.

Чащухин И.С., Вотяков С.Л., Щапова Ю.В. Кристаллохимия хромшпинели и окситермобарометрия ультрамафитов складчатых областей / ИГиГ УрО РАН. Екатеринбург, 2007. 310 с.

Чернышов А.И. Ультрамафиты (пластическое течение, структурная и петроструктурная неоднородность). Томск: Чародей, 2001. 215 с.

Чернышов А.И., Юричев А.Н. Петроструктурная эволюция ультрамафитов Калнинского хромитоносного массива в Западном Саяне // Геотектоника. 2013. № 4. С. 31-46.

Щербаков С.А. Пластические деформации ультрабазитов офиолитовой ассоциации Урала. М.: Наука, 1990. 120 с.

Ahmed Z. Stratigraphic and textural variations in the chromite composition of the ophio-litic Sakhakot-Qila Complex, Pakistan // Economic Geology and Bull. Soc. Econ. Geologists. 1984. Vol. 79. P. 1334-1359.

Arai S., Miura M. Podiform chromitites do form beneath mid-ocean ridges // Lithos. 2015. Vol. 232. P. 143–149.

Ballhaus C. Origin of the podiform chromite deposits by magma mingling // Earth and Planetary Science Letters. 1998. Vol. 156. P. 185-193.

Barnes S., Roeder P. The Range of spinel compositions in terrestrial mafic and ultramafic rocks // Journal of Petrology. 2001. Vol. 42. P.2279-2302.

Carter N.L. Steady state flow of rocks // Rev. Geophys. and Space Phys. 1976. Vol. 14. P. 301-360.

Cassard D., Nicolas A., Rabinowitch M., Moutte J., Leblanc M., Prinzhoffer A. Structural Classification of Chromite Pods in Southern New Caledonia // Economic Geology. 1981. Vol. 76. P. 805-831.

Dick H.J.B., Bullen T. Chromian spinel as a petrogenetic indicator in abyssal and Alpine-type peridotites and spatially associated lavas // Contrib Mineral Petrol. 1984. Vol. 86. P. 54-76.

Dickey J.S. A hypothesis of origin for podiform chromite deposits // Geochim. et Cosmochim. Acta. 1975. Vol. 39. P. 1061-1075.

Fedoseev V.B. Stratification of two-phase monodisperse system in a laminar planar flow // Journal of Experimental and Theoretical Physics. 2016. Vol. 149(4). P.1-11.

Franz L., Wirth R. Spinel inclusions in olivine of peridotite xenoliths from TUBAF seamount (Bismarck Archipelago/Papua New Guinea): evidence forthe thermalandtectonic evolution of the oceaniclithosphere // Contrib. Mineral. Petrol. 2000. Vol. 140. P. 283-295.

Gonzalez-Jimenez J.M., Griffin W.L., Proenza A., Gervilla F., O'Reilly S.Y., Akbulut M., Pearson N.J., Arai S. Chromitites in ophiolites: how, where, when, why? Part II. The crystallisation of chromitites // Lithos. 2014. Vol. 189. P. 148–158.

Gonzalez-Jimenez J.M., Proenza J.A., Gervilla F., Melgarejo J.C., Blanco-Moreno J.A., Ruiz-Sanchez R., Griffin W.L. High-Cr and high-Al chromitites from the Sagua de Tanamo district, Mayari-Cristal ophiolitic massif (eastern Cuba): Constrains on their origin from mineralogy and geochemistry of chromian spinel and platinum-group-elements // Lithos. 2011. Vol. 125. P.101-121.

Greenbaum D. The chromitiferous rocks of the Troodos ophiolite complex, Cyprus // Economic Geology. 1977. Vol. 72. P. 1175-1194.

Hock M., Friedrich G., Plueger W.L., Wichowski A. Refractory- and metallurgical-type chromite ores, Zambales Ophiolite, Luzon, Philippines // Mineralium Deposita. 1986. Vol. 21. P. 190-199.

Irvine T.N. Chromian spinel as a petrogenetic indicator. Part I: Theory // Canadian Journal Earth Science. 1965. Vol. 2. P. 648-672.

Kelemen P.B., Dick H.J.B., Quick J.E. Formation of harzburgite by pervasive melt/rock reaction in the upper mantle // Nature. 1992. Vol. 358. P. 635-641.

Kelemen P.B., Shimizu N., Salters V.J.M. Extraction of mid-ocean-ridge basalt from the upwelling mantle by focused flow of melt in dunite channels // Nature. 1995. Vol. 375. P. 747-753.

Kohlstedt D.L., Goetze C., Durham W.B., Sande van der J.B. A new technique for decorating dislocations in olivine // Science. 1976. Vol. 191. P. 1045-1046.

Kubo K. Dunite formation processes in highly depleted peridotite: case study of the Iwanaidake Peridotite, Hokkaido, Japan // Journal of Petrology. 2002. Vol. 43. P. 423-448.

Lago B.L., Rabinowicz M., Nicolas A. Podiform chromite ore bodies: a genetic model // Journal of Petrology, 1982, V. 23. P.103-125.

Leblanc M. Chromite Growth, Dissolution and Deformation from a Morphological View Point: SEM Investigations // Mineralium Deposita (Berl.). 1980. Vol. 15. P. 201-210.

Leblanc M., Violette, J.-F. (1983) Distribution of aluminium-rich and chromium-rich chromite pods in ophiolite peridotites // Economic Geology. 1983. Vol. 78. P. 293-301.

Matsumoto I., Arai S. Morphological and chemical variations of chromian spinel in dunite-harzburgite complexes from the Sangun zone (SW Japan): implications for mantle/melt reaction and chromitite formation processes // Mineralogy and Petrology. 2001. Vol. 73. P. 305-323.

Matveev S., Ballhaus C. Role of water in the origin of podiform chromitite deposits. Earth and Planetary Science Letters. 2002. Vol. 203. P. 235-243.

McElduff B., Stumpfl E.F. The chromite deposits of the Troodos complex, Cyprus - evidence for the role of a fluid phase accompanying chromite formation // Mineralium Deposita. 1991. Vol. 26. P. 307-318.

Melcher F., Grum W., Simon G., Thalhammer T.V., Stumpfl E.F. Petrogenesis of the ophiolitic giant chromite deposits of Kempirsai, Kazakhstan: a study of solid and fluid inclusions in chromite // Journal of Petrology. 1997. Vol. 38. P. 1419-1458.

Morishita T., Andal E.S., Arai S., Ishida Y. Podiform chromitites in the lherzolite-dominant mantle section of the Isabela ophiolite, the Philippines // Island Arc. 2006. Vol. 15. P. 84-101.

Nicolas A., Bouchez J.L., Boudier F., Mercier J.C. (1971) Textures, structures and fabrics due to solid state flow in some European lherzolites // Tectonophysics. 1971. Vol. 12. P. 55-86.

Prichard H.M., Barnes S.J., Godel B., Reddy S.M., Vukmanovic Z., Halfpenny A., Neary C.R., Fisher P.C. The structure of and origin of nodular chromite from the Troodos ophiolite, Cyprus, revealed using high-resolution X-ray computed tomography and electron backscatter diffraction // Lithos. 2015. Vol. 218–219. P. 87–98.

Proenza J., Gervilla F., Malgarejo J.C., Bodinier J.L. Al- and Cr-rich chromitites from the Mayari-Baracoa ophiolite Belt (Eastern Cuba): consequence of interaction between volatile-rich melts and peridotites in suprasubduction mantle // Economic Geology. 1999. Vol. 94. P. 547-566.

Roberts S. Ophiolitic chromite formation: a marginal basin phenomenon? // Economic Geology. 1988. Vol. 83. P. 1034-1036.

Thayer T.P. Principal features and origin of podiform chromite deposits, and some observations on the Guleman-Soridag District, Turkey // Economic Geology. 1964. Vol. 59. P. 1497-1524.

Yamamoto J., Ando J., Kagi H., Inoue T., Yamada A., Yamazaki D., Irifune T. In situ strength measurements on natural upper-mantle minerals // Phys. Chem. Minerals. 2008. Vol. 35. P. 249–257.

Zhou M.-F., Malpas J., Robinson P.T., Sun M., Li J.-W. Crystallization of podiform chromitites from silicate magmas and the formation of nodular textures // Resource Geology. 2001. V. 51. P. 1-6.

Zhou M.-F., Robinson P. High-Cr and high-Al podiform chromitites, western China: Relationship to partial melting and melt/rock reaction in the upper mantle // International Geology Review. 1994. Vol. 36. P. 678.